YEAR 2020-21

EXAM CANDIDATE ID:	**MXFY5**
MODULE CODE:	**NSCI0017**
MODULE NAME:	**Research Project**
SUPERVISOR	**Prof. Kwang Leong Choy** **Dr Mingqing Wang**
RESEARCH PROJCT TITLE:	**Preparation of Graphene Composite as Barrier coating for OTFT/OLED Active Matrix Displays**
WORD COUNT:	**……11644……**

Acknowledgements

Firstly, I want to say thank you to my supervisors. I want to thank Prof. Kwang Leong Choy for giving me advice and showing me the correct road when I am confused. Dr Mingqing Wang, she offered me great support during my experiment and study and was always there for me. Despite my lack of fundamental knowledge, she is always willing to guide me carefully. Talking to her was like talking to an old friend. I would like to send my sincere gratitude and best wishes.

Secondly, I want to thank my group mate, Yuhui and Nan. They supported me not only in laboratory but also in normal life. I am really happy to have such friends. Teachers and seniors in IMD are very kind and help me a lot with my experiment, making me feel the atmosphere like home. Thanks to all teachers teaching me knowledge, there is a Chinese saying goes, "once a teacher, always a father". I have learned so much from you for the rest of my life.

Lastly, I want to give special thanks to my parents. They keep silently supporting me, giving me the opportunity to study abroad. I cannot wait to see you after graduation.

One year is too short to say goodbye. Goodbye, dear teachers and classmates! Wish you all best and hope we can have a chance to meet each other again!

Table of Contents

1. Introduction ----- 5

2. Review

2.1 Comprehensive Introduction of OLED ----- 5

2.2 The Existing Main Problems of OLED

2.2.1 Problems in Technology Development ----- 8

2.2.2 Traditional Encapsulation Methods ----- 9

2.2.3 Introduction of Thin Film Technology ----- 9

***2.3 Application of Graphene and Its Derivatives in Barrier Polymer as Thin Film Encapsulation* ----- 11**

3. Methodology

3.1 Graphene

3.1.1 Characteristics and Properties of Graphene ----- 13

3.1.2 Synthesis of Graphene ------ 15

3.1.3 Barrier Mechanism of graphene and its derivatives ----- 16

3.2 Derivatives of Graphene

3.2.1 Characteristics and Properties of Graphene Oxide ----- 18

3.2.2 Synthesis of Graphene Oxide

3.2.2.1 Brodie Method and Staudenmaier Method of Graphite Oxide Synthesis -----20

3.2.2.2 Hummers Method of Graphite Oxide Synthesis ----- 20

3.2.2.3 Comparison of Synthesis Methods of Graphite Oxide ----- 20

3.2.2.4 Exfoliation of Graphite Oxide to Graphene Oxide ----- 21

3.2.2.5 Freeze Drying Technique ----- 22

3.2.2.6 Practical Experimental Method of Graphene Oxide Synthesis ----- 23

3.2.3 Characteristics, Properties and Synthesis of reduced Graphene Oxide ----- 25

3.3 Graphene / Polymer Nanocomposite

3.3.1 Introduction of Epoxy Resin ----- 27

3.3.2 Synthesis of Graphene/Polymer Nanocomposites ----- 29

3.3.3 Practical Experimental Method of GO/EP and rGO/EP Synthesis ----- 30

3.4 Preparation of Samples for Characterization* ----- 32

4. Results and Discussions

4.1 Film Thickness Measurement ----- 33

4.2 Contact Angle Measurement ----- 35

4.3 Transmittance Measurement ----- 36

4.4 X-ray Diffraction Patterns ----- 37

4.5 FTIR Spectrum of Graphene Oxide ----- 39

4.6 SEM Analysis ----- 40

5. Conclusions and Outlook ----- 41

6. Potential applications and socio-economic impact ----- 42

References ----- 43

Appendix ----- 50

Abstract

In this paper, a comprehensive review of development in encapsulation methods of OLED is delivered first. As 2 Dimensional(2D) materials, graphene and it's derivatives are supposed to form compact wall for water vapor and oxygen transmission. Application of graphene/its derivatives and their polymer composite as barrier coating is then studied in this work. The characteristics, properties and synthesis methods of graphene, graphene oxide (GO), reduced graphene oxide (rGO) as well as epoxy resin (EP) are summarized in detail. Modified Hummer's method is adopted for the synthesis of GO and solution mixing method is used to prepare GO/EP, rGO/EP nanocomposite solution in this study. The solution is then spin coated on glass and flexible substrates. By adjusting the rotating speed of spin coater, controlling of film thickness at nanometer scale is realized and verified using profiler. The influence of film thickness on transmittance of the barrier coating is discussed based on result from UV-Vis Spectrometer. All of the prepared films demonstrate high transmittance (>96%) at visible light range. Contact angle was used to characterize the surface hydrophilic/hydrophobic properties of the prepared films. XRD was used to compare the structures between natural graphite, GO and rGO. FTIR was used for the identification of functional groups in graphite oxide and SEM was used to check the surface morphology to make sure the prepared barrier coating is flat and without pin holes. The results indicate that many of graphene's superior properties have been saved to the GO/EP and rGO/EP nanocomposites film, which make this encapsulation technology attractive and promising.

Keywords: OLED, Graphene, Graphene Oxide, Epoxy Resin, Gas barrier, Polymer, Nanocomposites.

1. Introduction

Organic Light-Emitting Devices (OLEDs) have broad application prospects in display and lighting field due to their characteristics of wide colour gamut, wide viewing angle, high contrast, fast response, low power consumption and suitable for flexible substrates [1-3]. However, the industrialization of OLED technology still faces many difficulties to be solved. Organic materials and metal electricity in OLED are easily corroded by water vapor and oxygen in the air and lose their functions, which is one of the important problems hindering the development of OLED [4].

Due to its excellent electrical, mechanical and thermal properties, graphene, a monolayer of graphite, is being widely explored and has attracted great academic and industrial interest [5]. However, there are many problems with making graphene physically in industry, including defective graphene layers and difficulties in scale. Another way is to incorporate its derivatives including graphene oxide (GO) and reduced graphene oxide (rGO) into polymer matrix [6]. The gas barrier performance of polymer materials has become an important indicator in many applications, such as packaging, medicine, piping and electronics. Graphene and its derivatives have also been considered as superior nanoscale fillers in polymer nanocomposites for gas barrier applications, including encapsulation of OLED. In this study, Graphene Oxide (GO) and reduced Graphene Oxide (rGO) were prepared and incorporated into Epoxy Resin (EP) matrix respectively using solution mixing process to obtain EP based nanocomposites with enhanced gas-barrier properties. The GO/EP and rGO/EP solution was coated on glass and flexible substrates using spin coating technology and cured with UV light. The controlling of film thickness in nanoscale was realized and verified using profiler, thus 6 control groups with different thickness were set for measuring the effect of film thickness on transmittance and hydrophilia. XRD, FTIR and SEM are used for the material characterization.

2. Review

2.1 Comprehensive Introduction of OLED

Since the invention of OLED in 1987 by Dr. Qingyun Deng [6], OLED display technology has attracted extensive attention in the industry for its features such as wide colour gamut, high contrast, light and thin, large viewing angle, fast response speed, low power consumption, active light emitting mode without the need of backlight and can be prepared on flexible substrates [7-9].

Compared with existed mature technologies such as Liquid Crystal Display (LCD) and Light Emitting Diode (LED), although OLED has achieved initial success in intelligent electronics, TV and lighting [10], and it is superior to LCD and LED in terms of structure, contrast, response

speed and so on having a huge market demand its market share and penetration rate have not made great progress [11]. In particular, the industrialization of OLED is still facing great difficulties due to the problems in device life, device stability and yield [12-13]. These are all focused by current research in the industry. From the lighting principle of OLED, both organic small molecule devices based on dyes and pigments, and polymer devices based on conjugated polymers can be explained by the same theory. With the recombination of electrons and holes, an organic molecule with high energy state is formed. This state is called an excited state, and the molecule in the excited state is called an exciton. Excitons return from the excited state to the ground state by releasing energy, during which photons are emitted. Simply put, OLED is a technology that deposits a hole-injected anode and electron-injected cathode on a substrate, as well as organic materials that produce photons. Moreover, this technology is more attractive than any other display technology, because it can be prepared on a flexible substrate, which provides infinite possibilities for today's people who pursue colour and fashion in design [14], as shown in *Figure 1.*



Figure 1: OLED Technology Applications

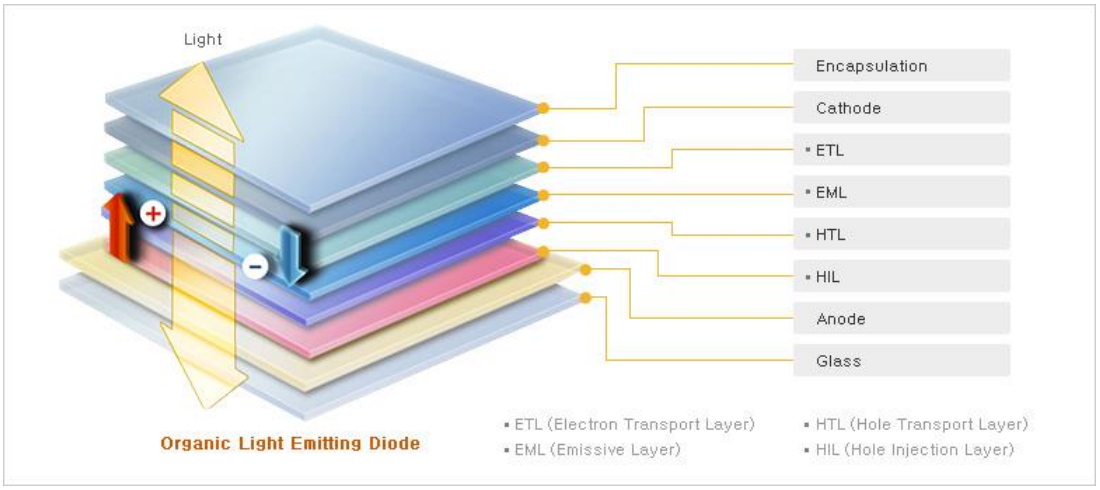


Figure 2: Schematic Structure of OLED

Modern OLED technology is basically a "sandwich" structure composed of organic layers with different functions [15]. The properties of each layer and its compatibility with adjacent materials

have a very important influence on the performance of OLED. The structure can be shown as *Figure 2.*

As can be seen from the *Figure 2,* there are mainly the following functional layers including [16]:

Hole Injection Layer (HIL)

The hole injection layer refers to the organic material layer inside the device by reducing the potential barrier that prevents the hole from being injected into the organic layer by the anode.

Hole Transportation Layer (HTL)

The hole transport layer refers to the organic material layer that transfers the hole injected from the anode to the luminescent layer.

Emission Layer (EML)

The luminescent layer is where the incoming holes and electrons combine. The holes and electrons reach the luminescent layer, find a docking charge for each other, and recombine. By stripping electrons from otherwise neutral organic molecules or injecting holes, the electrons and holes recombine in the luminescent layer, reducing the organic material in its excited state to neutral molecules. From the molecular state, the electron from the ground state to the high energy excited state, the excited state is extremely unstable, and then back to the ground state, this process energy is released in the form of "light".

Electron Transportation Layer (ETL)

The electron transport layer transmits electrons to the luminescent layer, and at the same time blocks the hole transfer to the cathode, so that the charge meets and recombines in the luminescent layer. Similar to the hole transport layer, the electron transport layer material should have a wider energy gap than the luminescent layer.

Electron Injection Layer (EIL)

The electron injection layer enhances the cathode electron injection capability. However, when the work function of the electron transport layer and the cathode material match, the electron transportation Layer can be used directly without using electron injection layer.

During the process of device preparation, the technologies used for small molecule organic materials and polymer organic materials are different. At present, the popular market is mostly small molecular organic materials, the thickness of each organic layer is about 20~50nm [17]. Therefore, in theory, OLED devices could be made very thin, or even transparent and flexible. This unparalleled technological advantage is destined to enable OLED technology to show extraordinary talents in the display and lighting field.

2.2 The Existing Main Problems of OLED

2.2.1 Problems in Technology Development

When OLED was first developed, it was widely regarded as the most promising next generation display lighting technology. OLED has many advantages over mature LCD and LED technologies. However, there are still many technical problems waiting to be solved in OLED [18].

(1) Large-area OLED Display

OLED has achieved great success in small area display, especially in small electronic products such as mobile phones, but the production of large area display has always been a difficult subject. Many companies have hit a brick wall with OLED TVS so far [19].

(2) Short Service Life

OLED is very sensitive to water and oxygen in the air, especially water vapor in the air. The reason is that the organic layer is easy to react with water vapor and oxygen in the air, resulting in changes in the structure and performance of the material, thus losing its original role and forming dark spots on the surface of the device. Therefore, encapsulation technology is particularly important for the development of OLED technology. In order to meet the requirements of production, OLED devices are required to have a service life of more than 10,000 hours and a storage life of more than 50,000 hours [20]. The Water Vapour Transmission Rate (WVTR) of encapsulation should be controlled under $5 \times 10 - 5\ g/m^2/day$, which requires high barrier performance of the device [21].

(3) Lack of Stability

Due to the high requirements of OLED devices and materials, even a little defect will cause serious damage to the whole device [22]. At present, organic materials are still not mature, after a long time of use, some materials will appear the phenomenon of recrystallization. Moreover, the life of red, green and blue luminescent materials is also very different, which leads to some distortion in the display device for a period of time [23].

Although OLED has encountered some difficult difficulties, its development trend and prospects are still bright, and a large number of scientists are trying to solve these problems.

2.2.2 Traditional Encapsulation Methods

It has been emphasized that water vapor in the air and oxidation of oxygen are an important factor contributing to rapid device degradation. Therefore, effectively encapsulating OLED to

prevent water vapor and oxygen from entering into the device is an important technology to solve OLED degradation [24]. Traditional glass encapsulation technology is to use glass or metal cover plate, through epoxy resin and device bonding together [25]. The entire encapsulation process is carried out in an environment filled with inert gas (e.g., Argon, Nitrogen, etc.), so that a closed space is formed between the device and the glass cover plate and is isolated from the external environment [26]. However, the glass and metal cover plates are made of steel materials, and the three-dimensional network structure formed by epoxy resin curing is easy to crack, which leads to water vapor infiltration and affects the sealing performance of the device [27-28]. Therefore, desiccant (CaO) is often added to the interior of the packaged device to absorb water vapor entering the device through the interface. When the desiccant absorbs a certain amount of osmotic water vapor, it expands, which affects the performance of the device. Currently, the glass-based AMOLED packaging technology is FRIT packaging, which still uses glass [29]. The so-called FRIT packaging technology is a packaging technology that uses laser irradiation to instantly melt glass powder containing oxides (e.g., $V_2O_5/P_2O_5/Fe_2O_3/TeO_2/BaO/SiO_2/PbO/SnO$, etc.) and glass slurry raw materials, so that the upper and lower glass plates are bonded together [30]. Obviously, this traditional glass cover plate packaging structure will increase the weight of the device, and the cover plate itself is not flexible. Therefore, this packaging method cannot meet the requirements of flexible packaging [31].

2.2.3 Introduction of Thin Film Technology

Thin Film Encapsulation mainly uses film covering, which is deposited on the surface of the device. If a flexible substrate is used, the front and back sides should be enclosed to isolate the device from air due to the limited water and oxygen resistance of the flexible substrate. The key to this encapsulation method lies in the barrier ability of the encapsulation film to water and oxygen. In order to meet the commercial requirements, OLED packaging film of water and oxygen barrier ability to put forward high requirements. High mechanical strength, optical transparency, thermal and chemical stability should also be required for ideal packaging [32].

At present, there are many methods to improve the barrier performance of polymer materials as thin film encapsulation, but they still have some disadvantages, including high cost, high humidity, sensitivity, opacity and low mechanical strength. The most common approach is to coat thin film polymers using low permeability barrier polymers such as polyethylene (PE), polypropylene (PP), and polyvinyl alcohol (PVA), etc [33]. However, although such polymers are light, inexpensive and easy to process, their use as barriers is often limited by their relatively high permeability compared to the high standards of modern packaging applications. *Figure 3(a)* shows water vapor transmittance (WVTR) and oxygen transmittance (OTR) for common organic polymers used in barrier applications [34]. It can be seen that the vapor barrier

performance of some polymers only meets the food packaging standards. They are far from enough for current display devices, including OLEDs and LCDS.

Another promising technology is inorganic and organic hybrid thin film encapsulation. Inorganic films have high water vapor isolation ability and can often be used as a water-blocking layer. However, defects (e.g., pinholes, cracks, etc.) will inevitably occur in the process of forming inorganic thin films, and the existence of defects greatly reduces its barrier ability [35]. In addition, too many or too thick inorganic layers will produce large internal stress, seriously affect the package quality. The study shows that the organic - inorganic interlaced packaging method can reduce the defects and stress of inorganic film. At present, the organic/inorganic hybrid thin film encapsulation technology developed by Vitex System [36] is widely used in the field of film packaging, as shown in *Figure 4(a).* There are nine inorganic organic structures with a total thickness of 3~4 μm. It is also called Barix film packaging technology [37]. In fact, the organic layer only plays a role in improving the sample surface flatness and reducing mechanical loss, only the inorganic packaging layer really plays a role in packaging.

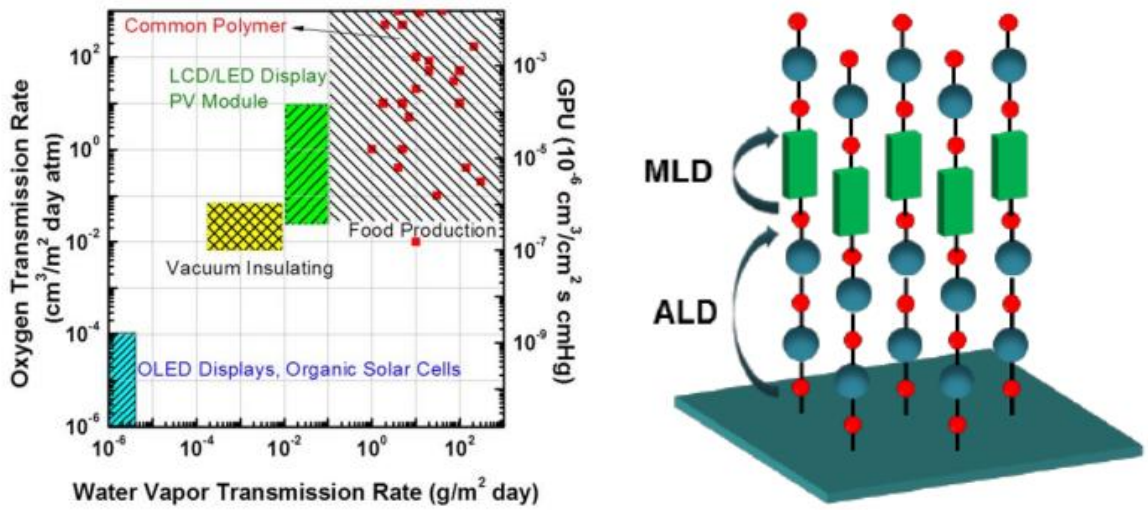


Figure 3: (a) [34] *Water vapor transmittance (WVTR) and oxygen transmittance (OTR) for common organic polymers used in barrier applications. (b)* [39] *ALD/MLD preparation of hybrid inorganic/organic thin film.*

Figure 4(b) shows the packaging method adopted by Samsung, South Korea [38]. CVD is used to deposit inorganic silicon nitrite film and inkjet printing sandwich structure of organic materials, with a total thickness of 8-10um and a fast-packaging rate, which can be used for flexible OLED technology packaging. Meanwhile, CVD technology is relatively mature and suitable for industrial production. But the film made by CVD is easy to crystallize and the packaging effect is not very ideal. Chen et al. [39] use ALD or MLD to prepare amorphous films shown in *Figure 3(b)*. This kind of multilayer thin film exhibits extremely low WVTRs, making it ideal for use as

an OLED protective layer. However, ALD and MLD are expensive and their wide use is still limited.

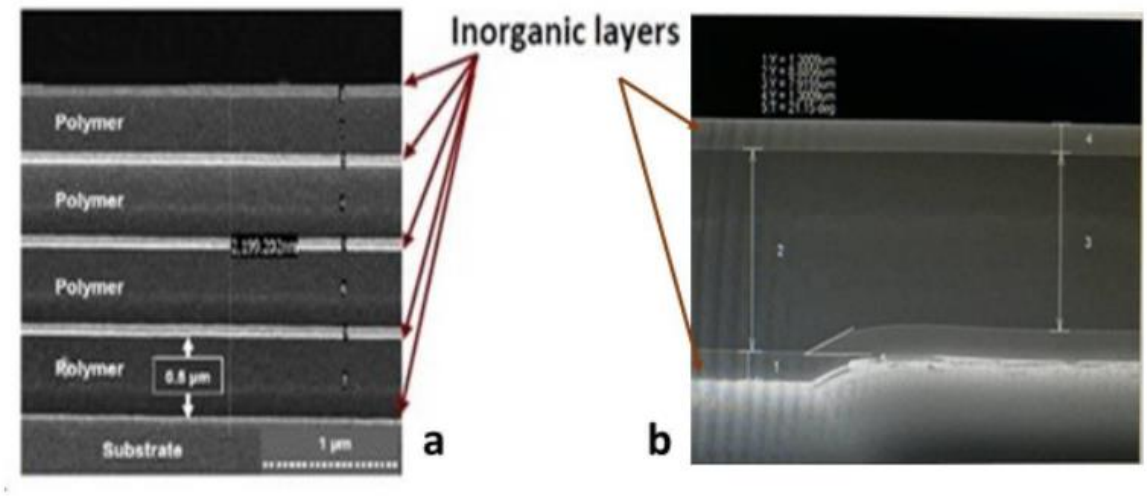


Figure 4: Common thin film encapsulation methods of OLED.

(a) [37]: Barix encapsulation; (b) [37]: CVD/Inkjet/CVD encapsulation.

2.3 Application of Graphene and Its Derivatives in Barrier Polymer as Thin Film Encapsulation

The gas barrier performance of polymer materials has become an important indicator in many applications, such as packaging, medicine, piping and electronics [40-44]. Due to its easy processing, light weight, low cost and multifunctional characteristics, polymer materials used for gas barrier gradually replace the traditional materials, such as polyethylene, poly (propylene), polystyrene, polyvinyl chloride, poly (lactic acid) and polyvinyl alcohol, the most commonly used polymer materials in the packaging industry [45-47]. However, the relatively high gas permeability of most polymer materials limits their use in applications. Therefore, it is necessary to research and develop how to improve the barrier of polymer materials while maintaining good mechanical properties and processing characteristics and meeting the needs of modern industrial applications.

The gas permeation mechanism of polymer materials consists of three distinct steps: physical adhesion of gas to the surface of polymer materials, absorption of adherent gas molecules, and diffusion of gas in polymer materials. Therefore, adding impermeable layered fillers, such as organic montmorillonite, mica and graphene nanosheets, into the polymer matrix is an effective means to improve the gas barrier performance of polymer materials. These fillers can form "nano barrier walls" in the polymer matrix, which can change the diffusion path of gas permeable molecules in the polymer and make the diffusion molecules follow a longer and more tortuous path through the nanocomposite membrane [48]. As shown in the *Figure 5, Figure 5(a)* shows polymer only, and *Figure 5(b)* shows after adding non-porous nanomaterials into

the polymer matrix [49]. In this process, there are three main factors affecting the bending of the diffusion path of the diffusion molecule: the mass fraction of the nanosheet, the morphology of the nanosheet, and the specific surface area of the nanosheet. Therefore, uniformly dispersed nanosheets with large specific surface area are ideal structures for preparing nanocomposite films with high gas barrier.

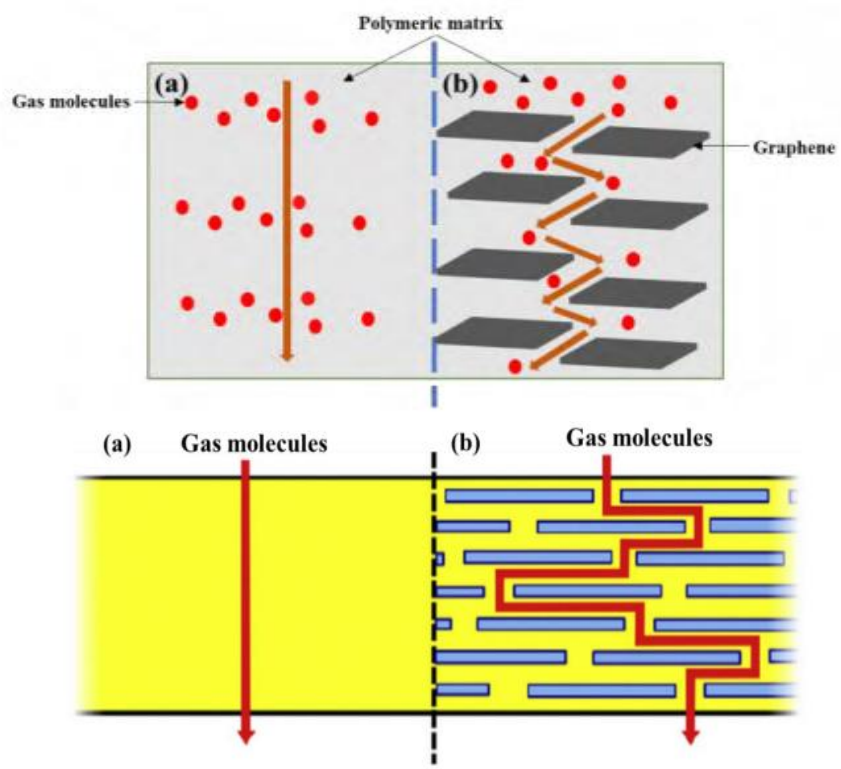


Figure 5 [49]: Illustration of the tortuous pathway created by incorporation of exfoliated nanoplatelets into a polymer matrix film. (a) Polymer only; (b) Nanocomposite.

Montmorillonite and mica sheet are widely used as nanofillers in polymer composite barrier applications because of their high specific surface area and good compatibility with various polymers. Compared with montmorillonite and mica sheets, graphene blends with polymers not only show better gas barrier properties, but also better mechanical strength, electrical conductivity and thermal properties when properly dispersed in the polymer matrix. Kalaitzidou et al. [50] found that graphene and GO were significantly better than nanocomposites such as carbon nanotubes, carbon black and montmorillonite in improving the gas barrier of polymer materials. Compared to other carbon nanoparticles, such as carbon nanotubes and fullerenes, graphene has a high surface to volume ratio, allowing for the longest gas diffusion path even at low volumes.

In recent years, graphene has attracted extensive attention due to its superior material properties and has become one of the most widely studied materials [51]. In addition, graphene, a mono layer of graphite, is thought to be an ultra-thin, perfectly two-dimensional (2D) barrier against the diffusion of gases. Ideally, defectless single crystal monolayer graphene not only

has excellent mechanical properties and high transparency, but also is impermeable to air. However, the synthesis of large-area, defection-free, single crystal, monolayer graphene remains extremely challenging [52-55]. One strategy to exploit graphene's gas impermeability properties in mass production is to use Graphene Oxide (GO) and its reduced form Reduced Graphene Oxide (rGO) [56]. GO consists of oxygen-containing functional groups on the base plane that disperse well in polar solvents such as water, leading to scalable mass production. However, there are some defects in the GO base plane. Therefore, multi-layer, highly interlocked deposits would be preferred. Unfortunately, GO is significantly affected by relative humidity due to its hydrophilicity and is subject to thermal shock even at low temperatures due to its structural instability. Therefore, the deposited graphene oxide film layer should be chemically or thermally reduced to prevent water vapor from penetrating or absorbing water on its surface [57]. In the process of reduction, it is necessary to solve the problem of easy damage to the surface of OLED, which is not conducive to large-scale economic production. Therefore, another approach is to mix graphene and its derivatives, including GO, rGO and functionalized GO (FGO) or functionalized Graphene (FG) nanosheets physically or chemically with polymers to prepare graphene/polymer nanocomposites.

3. Methodology

As mentioned above, the research focus of this paper will be on the preparation of nanocomposites by mixing graphene and its derivatives with polymers. In this chapter, the properties, characteristics, structures and barrier mechanism of graphene and its derivatives will be carefully and comprehensively described. Their preparation methods will also be discussed in detail. Epoxy resin, which is chosen in the research of this paper to make graphene/polymer nanocomposites, will then be fully expounded.

3.1 Graphene

3.1.1 Characteristics and Properties of Graphene

Graphene was developed in 2007 by Physicists Geim and Novoselov [58] of the University of Manchester in the United Kingdom by separating natural graphite into smaller pieces and taking thinner parts from the resulting graphite fragments, which is illustrated in the *Figure 6*. The advent of graphene has caused a worldwide research boom. Electrons in graphene behave like relativistic massless particles, but follow linear diffusion laws, which allow graphene to exhibit many peculiar electrical properties, such as the quantum Hall effect and excellent light transmission. Because of graphene's extremely high carrier mobility $(200000 cm^2/Vs)$, thermal conductivity $(\frac{3000W}{mk})$ and electrical conductivity, graphene

electrodes can revolutionize complementary Metal Oxide Semiconductor (MOS) electronics [59].

Graphene is considered to be a soft, two-dimensional crystalline material that is impervious to any gaseous molecule, as demonstrated and experimented in molecular simulations. The electron density of the aromatic rings in graphene is high enough to repel the penetration of atoms or molecules. For example, energy barriers form when a single-atomic molecule, such as Helium (He), approaches the center of a defection-free graphene monolayer carbon ring. The energy barrier calculated with the Local Density Approximation (LDA) is about 18.8eV. The kinetic energy of the He atom (18.6 eV) is less than the 18.8eV required to penetrate the barrier. Relaxation of the graphene layer begins only after He atoms are reflected. This is nicely illustrated in the *Figure 7* [34]. Therefore, defectless monolayers of single crystal graphene can act as a good barrier to gas transport at room temperature. However, it is difficult to synthesize large, defection-free graphene sheets because graphene boundaries, point defects and carbon rings contain more or less than six carbon atoms.

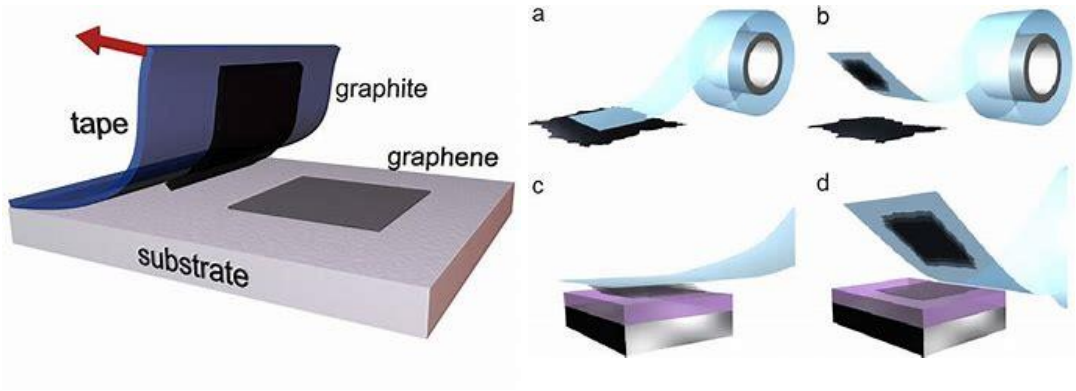


Figure 6: The invention process of Graphene

Graphene is a single layer of carbon atoms in a cellular structure formed by a single carbon atom hybridizing in SP^2 with bonds to three adjacent carbon atoms, as shown in the *Figure 7(b)*. Because graphene with complete structure is a two-dimensional crystal composed of stable benzene six-membered rings, it has high chemical stability. Graphene is a surface inert material with weak interfaces with polymers. Moreover, the strong van der Waals force between the graphene sheets makes it easy to produce irreversible aggregation in the polymer matrix, which makes it extremely difficult to prepare various graphene composite materials for research and application [61]. In addition, graphene is neither hydrophilic nor oleophilic, making it difficult to disperse evenly in the polymer matrix and unable to dissolve into other solvents, resulting in moulding difficulties. Therefore, it is usually necessary to modify graphene. By introducing some specific functional groups into the ring structure of graphene, specific properties can be given to graphene to improve the dispersion and compatibility of graphene in the polymer matrix. At present, the most common way to modify graphene is to obtain

graphene oxide (GO) after functionalization, because GO has a similar structure to graphene. The oxygenation reaction only makes the GO lamellar surface with many oxygen-containing functional groups such as hydroxyl, carboxylic group and epoxy group [62], so as to improve its dispersibility in organic solvents and polymer matrix and enhance compatibility with polymer matrix. This makes it better applied in the field of composite materials, thus helps improving the performance of composite materials in all aspects [63].

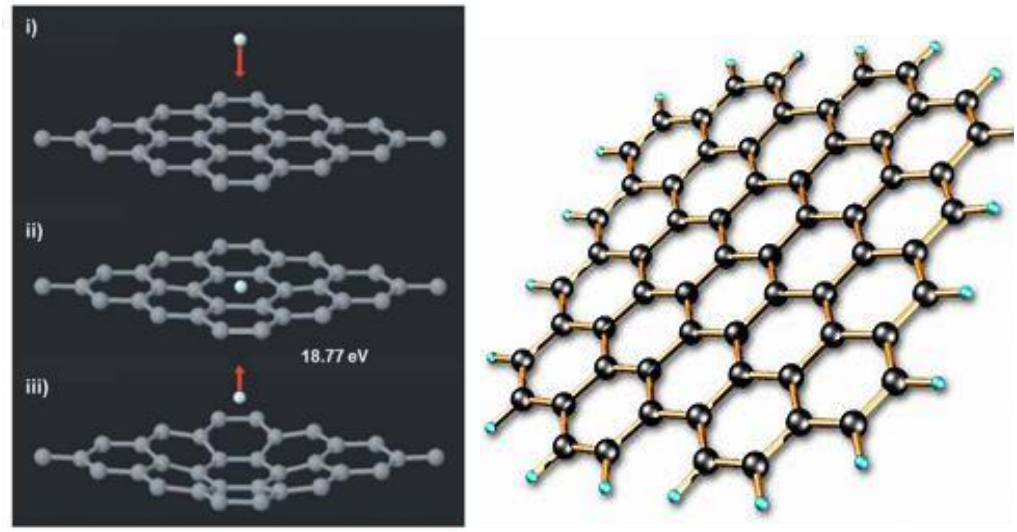


Figure 7(a) shows the reflection of He atom with kinetic energy of 18.6 eV on graphene surface. i) He atom is getting closer to perfect graphene layer. ii) He atom rests before penetrating the graphene layer; iii) The He atom is reflected back and the surface begins to relax. [Reproduced from ref. 60]

Figure 7(b) shows the monolayer of carbon atoms with a cellular structure.

3.1.2 Synthesis of Graphene

In order to prepare large area defection-free graphene monolayers, many synthetic methods have been explored. These methods can be roughly divided into physical methods and chemical methods. Physical methods include mechanical exfoliation and large wafer transfer-printing method. Initially, graphene was prepared by mechanical exfoliation, but this method could only produce small amounts of graphene, which could not be mass-produced, and it was difficult to control the size of monolayers, which limits its application. Chemical methods include epitaxial growth, chemical vapor deposition and graphite oxide reduction [64]. Depending on the preparation method, different types of graphene can be prepared, including size, degree of exfoliation, purity and structural defects [65]. Among these methods, CVD growth method is the most suitable for obtaining high-quality graphene considering the cost [66]. However, graphene in the CVD method has many defects that may lead to adverse molecular transport. In the early stage of CVD, grain boundaries between single-crystal graphene domains are formed by connections between isolated graphene islands during growth. These

grain boundaries of polycrystalline graphite dominate gas transport with unfavourable molecular transport. In addition, graphene synthesized by CVD tends to have inherent defects (1-15nm in size) [67]. In other words, it is difficult to make defect-free, perfect graphene. Graphene can be produced in large quantities by the graphite oxide (GO) reduction method. However, some properties of graphene, such as electrical conductivity, may be lost as the graphite oxide may not be completely reduced. Currently, there have been many studies on large-scale preparation of high-quality defect-free graphene based on theoretical methods. However, due to current technological limitations, there are many prerequisites for the synthesis of perfect graphene with theoretically desirable properties. In the future, therefore, there is a need to develop technologies to grow perfect graphene, defection-free transfer methods, nanopore tuning techniques with advanced electron beam resolution, and simple multi-layer stacking techniques [68].

3.1.3 Barrier Mechanism of graphene and its derivatives

As mentioned in *Chapter 2.3* of this paper, graphene as filler can form a "nano barrier wall" in the polymer matrix, thus changing the diffusion path of gas permeable molecules in the polymer, making the diffusion molecules pass through the nanocomposite membrane along a longer and more tortuous path. The barrier mechanism of graphene/polymer nanocomposites can be explained by the theoretical model of small molecule permeability, which began in the 1960s, about 20 years earlier than experimental studies [69]. The molecular permeability theoretical model assumes that layered nanocomposites are composed of small molecule permeable phase (polymer matrix) and small molecule impenetrable phase (layered nanofiller). The nano lamellae generally have a uniform shape and are regularly arranged and dispersed in the matrix at an Angle to the direction of small molecule penetration. The model shows that the main factors affecting the barrier property of layered nanocomposites are the mass fraction of lamellar filler, the specific surface area of lamellar filler and the angle between lamellar filler and small molecule permeation direction. Nielsen [70] proposed a simple model of a polymer matrix containing a regularly arranged inorganic plate, as shown in the *Figure 8*. The watertight inorganic platelets in a permeable polymer matrix can create much more tortuous and longer paths for the diffusion of gas molecules.

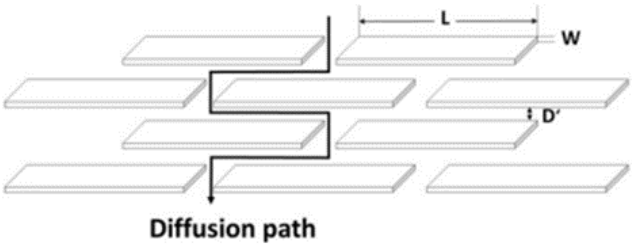


Figure 8 [70]: Schematic diagram for numerical calculation

The penetration of gas molecules into the polymer matrix conforms to the "dissolution-diffusion" theory, and the steady-state diffusion process of gas molecules conforms to Fick's first diffusion law:

$$q = -D\frac{dc}{dx} \quad (1)$$

Where,

$\frac{dc}{dx}$ represents gas concentration, the unit is kg/m^4;

D represents diffusion coefficient, the unit is d;

q represents gas transmission in unit time and unit area, the unit is $kg/m^2 s$.

The process of gas molecule dissolution conforms to Henry's law

$$C = S \cdot p \quad (2)$$

Where,

C represents the mole fraction of gas dissolved in polymer matrix in unit volume, the unit is mol/m^3;

p represents ambient pressure, the unit is Pa;

S represents solubility coefficient, the unit is $mol/m^3 Pa$.

Osmotic coefficient P_g is used to quantitatively characterize the complexity of the gas molecule passing through the nanocomposite thin film:

$$P_g = D \cdot S \quad (3)$$

Where, P_g represents osmotic coefficient, the unit is $mol/m \cdot s \cdot Pa$.

According to $equation\ (3)$, the decrease of both solubility coefficient S and diffusion coefficient D will make the nanocomposite thin film's Osmotic coefficient decrease.

After the addition of nanosheets, the mass of polymer matrix decreases and results in the decrease of solubility coefficient S of small molecules in nanocomposites, which can be expressed by the $equation\ (4)$:

$$S = S_0(1 - \omega)\ (4)$$

Where,

S_0 represents the solubility coefficient of small molecules in matrix, the unit is $mol/m^3 Pa$;

ω represents the mass fraction of the nanosheet layer.

At the same time, the addition of nanosheets as impermeable filler forces the infiltration path of small molecules to become longer and more tortuous. And this in turn leads to a decrease in the diffusion coefficient D, which can be expressed by the $equation\ (5)$:

$$D = \frac{D_0}{\tau} \ (5)$$

Where,

D_0 represents the diffusion coefficient of small molecules in matrix, the unit is m^2/s;

τ represents the tortuosity, and it is decided by the specific surface area, shape and orientation of the nanosheet, which can be expressed by the $equation\ (6)$:

$$\tau = \frac{l'}{l_0} \ (6)$$

Where,

l' represents the length of the path that a small molecule takes through the film;

l_0 represents the thickness of the film.

The $equation\ (7)$ can be obtained by the combination of $equation\ (3)$, $equation\ (4), equation\ (5)\ and\ equation\ (6)$:

$$\frac{P}{P_0} = \frac{1-\omega}{t} \ (7)$$

Where,

P represents the osmotic coefficient of the nanocomposite, the unit is $mol/m \cdot s \cdot Pa$;

P_0 represents the osmotic coefficient of the polymer matrix, the unit is $mol/m \cdot s \cdot Pa$;

The decrease of the diffusion coefficient D becomes the key step to control the decrease of the osmotic coefficient P, because the additional amount of nanosheets is usually very low and the mass fraction ω is very small, and the decrease of the polymer matrix mass can be ignored. Therefore, τ becomes the main factor affecting the barrier performance. So far, the barrier mechanism of graphene has been explained clearly.

When graphene nanosheets are not added to the polymer matrix, gas molecules can directly penetrate from one side of the film to the other side. However, when graphene nanosheets are added, the gas molecules can only penetrate through the defects due to graphene's blocking effect. The permeability path of gas molecules is lengthened and the tortuosity τ is increased, which makes the gas permeability coefficient of nanocomposites reduced, and the effect of graphene on enhancing the gas barrier performance of polymer is achieved. Last but not least, the derivatives of graphene including GO, rGO share the same mechanism with graphene [71].

3.2 Derivatives of Graphene

3.2.1 Characteristics and Properties of Graphene Oxide

As mentioned before in the *Chapter 2.3 and 3.1.1*, the synthesis of large-area, defection-free, single crystal, monolayer graphene remains extremely challenging [72]. In addition, graphene itself has low processability with conventional polymers and solvents in the chemical process,

and it is difficult to disperse evenly in the polymer matrix and cannot dissolve into other solvents. Therefore, it is usually necessary to modify graphene. By introducing some specific functional groups into the ring structure of graphene, specific properties can be given to graphene to improve the dispersion and compatibility of graphene in the polymer matrix. In contrast, graphite in solution as a precursor of graphite chemical graphite oxide is easy to produce in bulk, and the chemical graphite oxide itself has high processability. Therefore, one strategy to exploit graphene's gas-resistance properties in mass production is to use graphene oxide (GO), which can be considered as chemically functionalized graphene containing oxygen groups, and its reduced form reduced graphene oxide (rGO) [73]. In fact, the preparation of graphite oxide from natural graphite has long been considered a strategic starting point for large-scale synthesis of graphene.

Graphite oxide is a product of strong oxidation and hydrolysis of highly crystallized graphite, which can be incorporated into a class of graphite interlayer compounds with covalent bonds [74]. The structure of GO is similar to graphene, except that there are some oxygen-containing functional groups attached to the two surfaces and edges. These functional groups are mainly hydroxy, epoxy, dial and spindle groups, where the hydroxy and epoxy groups are located on the basal plane of GO, while dial and spindle groups are mainly distributed on the edge of GO, as shown in *Figure 9*.

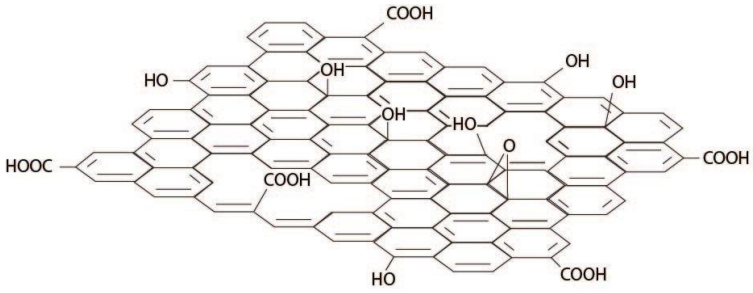


Figure 9: Schematic model of a sheet of graphene oxide

As described above, GO actually adds some oxygen-containing functional groups to the base plane and edge of graphene. The presence of these oxygen-containing functional groups destroys the graphene's conjugate bond structure, causing GO to lose its electrical conductivity and become an insulator [75]. On the other hand, due to the presence of oxygen-containing functional groups, GO is hydrophilic and has good dispersion in water. Li et al. suggested that the hydroxyl and carboxy groups contained in GO would be ionized in water, giving it a negative charge and electrostatic repulsion, thus dispersing evenly in water. In his opinion, the good dispersion of GO in water is not only due to the hydrophilicity of its oxygen-containing functional groups, but also due to the electrostatic repulsion between GO sheets. According to Lerf et al [76], in most cases, the epoxy and hydroxyl groups are thought to be on the base plane, while the carbonyl and carboxylic acid groups are on the edges, shown as the *Figure 9*. After much

research, the exact chemical structure of GO is still being explored. Compared to graphene, the oxygen functional groups in GO cause some structural defects. However, in some polar solvents, especially in high pH water without any surfactants, the edge carboxylic groups of GO suspensions help stabilize the colloidal state electrostatically. Post treatment such as ultrasonic treatment and further centrifugation may be necessary to achieve complete abscission of the GO suspension. The monolayer thickness of GO is about 1-1.4 nm thicker than monolayer graphene (0.34 nm) because of the oxygen-containing functional groups on the base plane [77].

3.2.2 Synthesis of Graphene Oxide

3.2.2.1 Brodie Method [78] and Staudenmaier Method [79] of Graphite Oxide Synthesis

Graphite Oxide is usually prepared from graphite oxide. Graphite can be thought of as being made of graphene stacked in space, and then graphene oxide stacked into graphite oxide. Graphite oxide was first discovered by Brodie in 1859 when he was studying the structure of graphite. In one experiment he added potassium chlorate $(KClO_3)$ to natural graphite mixed with fuming nitric acid (HNO_3). At the end of the reaction, it was confirmed that the resulting substance was composed of carbon, hydrogen and oxygen elements, which is why the substance has increased in weight compared to the graphite before the reaction.

Forty years after the first discovery that graphite could be oxidized, Staudenmaier improved the method of graphite oxide. In addition to oxidizing graphite with potassium chlorate, he added concentrated sulfuric acid to the reaction system to make the mixture more acidic. The oxidation degree of products obtained by Staudenmaier's method is basically the same as that of Brodie's method, but his method can be basically completed in one time in the same system.

3.2.2.2 Hummers Method [80] of Graphite Oxide Synthesis

Sixty years after Brodie's method appeared, Hummers developed a new method of oxidation. By reacting graphite with potassium permanganate $(KMnO_4)$ and concentrated sulfuric acid(H_2SO_4), he obtained graphite oxide with an oxidation degree similar to Brodie's graphite oxide. Although these reaction methods have been slightly modified by later generations, these three methods are basically the main way to synthesize graphite oxide.

3.2.2.3 Comparison of Synthesis Methods of Graphite Oxide

There are great differences in the reaction products in these methods. Actually, these differences are not only related to the oxidizer used, but also related to the graphite raw materials and reaction conditions. Both Brodie and Staudenmaier methods use potassium chlorate as an oxidant and mix graphite, potassium chlorate, and fuming nitric acid then

conduct processing. Nitric acid is a common oxidant and can react strongly with aromatic groups on carbon, including carbon nanotubes [81]. When nitric acid reacts with the aromatic groups, the aromatic groups are introduced into various oxygen-containing groups including carboxyl, lactone and ketone groups [82]. Likewise, potassium chlorate is a strong oxidizer commonly used in explosive materials. Potassium chlorate is a typical in situ source of dioxygen as reactants in the reaction, mainly plays an oxidation role in the strong oxidation reaction. The Hummers method uses potassium permanganate and sulfuric acid to oxidize graphite. Although permanganate is also a common oxidant, the actual reaction in the process is manganese heptoxide (Mn_2O_7). The reaction chemical equation can be expressed by *equation (8)*:

$$KMnO_4 + 3H_2SO_4 \rightarrow K^+ + {MnO_3}^+ + H_3O^+ + 3{HSO_4}^-$$

$${MnO_3}^+ + {MnO_4}^- \rightarrow Mn_2O_7 \quad (8)$$

The dark red oily substance, manganese heptoxide (Mn_2O_7), is produced by the reaction of potassium permanganate with sulfuric acid. This kind of bimetallic heptoxide is much more reactive than the mono-metal peroxide complexes and can explode when the temperature of the system exceeds a certain temperature or when it comes into contact with organic compounds [83]. The methods used in the literature and comparison between them are summarized in *Table 1* in the next page.

3.2.2.4 Exfoliation of Graphite Oxide to Graphene Oxide

Whereas graphite is thought of as a material with a three-dimensional structure made up of innumerable graphene sheets stacked together, graphite oxide can be thought of as a material made up of innumerable graphene sheets stacked together by van der Waals forces. If graphene and GO are to be prepared, the van der Waals forces between these sheets need to be broken. Thermal expansion method is commonly used to prepare graphene, while ultrasonic exfoliation method is usually used to prepare GO [87]. Ultrasonic exfoliation involves dispersing graphite oxide in deionized water and then ultrasonic treating the mixture using instruments such as an ultrasonic cleaning machine or an ultrasonic cell crusher. A typical ultrasonic instrument used during the experiment of this paper is shown in the *Figure 10(a)*. The process is simple and safe. During the ultrasonic process, the ultrasonic wave radiates in the graphite oxide suspension in dense and alternating intervals, thus making the liquid flow and producing a large number of bubbles. Ultrasonic wave is a longitudinal wave, and these bubbles will grow on the negative pressure formed in the direction of the ultrasonic wave and close in the positive pressure area, which is called "cavitation" effect. In the "cavitation" effect, the closure of bubbles creates an extremely high transient pressure, which continuously shocks

the GO sheets and breaks the van der Waals force connections between the sheets, thus causing the GO sheets to break free from the van der Waals force and fall off [88].

Method	*Oxidants*	*Solvent*	*Oxidation time*	*Advantages*	*Disadvantages*	*Reference*
Brodie	$KClO_3$	HNO_3	*3 days*	*Stable, Low pollution, Small interlayer distance.*	*Slow, Complex operation (Need multiple reactions).*	*78*
Staudenmaier	$NaClO_3$	HNO_3	*2 days*	*Complete Structure, Controllable degree of oxidation*	*High risk, Slow.*	*84*
Hummers	$NaNO_3$ $KMnO_4$	H_2SO_4	*1 hour*	*Fast reaction, Fewer defects, High degree of oxidation, Safer.*	*High pollution (H_2SO_4), Degradation.*	*80*
Modified Hummers	P_2O_5 $KMnO_4$	H_2SO_4	*8 hours*	*Safer, Less pollution (Compared to Hummers).*	*Relatively slower (Compared to Hummers).*	*85*
	$KMnO_4$, Mn_2O_7	H_2SO_4 H_3PO_4	*15hours*			*86*

Table 1: Comparison between GO synthesis methods

3.2.2.5 Freeze Drying Technique

Freeze drying is also called sublimation drying. It is a drying method that freezes the water-bearing material below freezing point, turns the water into ice, and then removes the ice into vapor under a higher vacuum. The material can be frozen in the freezer first and then dried. It can also be frozen directly in the drying chamber by rapid vacuum pumping. The steam

generated by sublimation is removed by the condenser. The vaporization heat required in the sublimation process is generally supplied by thermal radiation [89].

Because vacuum freeze drying is carried out at low temperature and low pressure, and water sublimates directly, it gifts the product many special properties. For example, vacuum freeze drying technology can dehydrate heat-sensitive materials more thoroughly, and the dried drugs are very stable, easy to store for a long time. Compared with other drying methods, the physical structure and molecular structure of materials have little change, and their organizational structure and appearance are well preserved. In the vacuum freeze drying process, the material does not have the problem of surface hardening, and its internal formation of porous spongy, therefore it has excellent rehydration, thus can be restored to the state before drying in a short time. Because the drying process is carried out at a very low temperature, and basically isolated from the air, it effectively inhibits the biological, chemical or physical changes of heat sensitive substances, and better preserves the active substances in the raw materials. A typical freeze drying instrument used during the experiment of this paper is shown in the *Figure 11*.

3.2.2.6 Practical Experimental Method of Graphene Oxide Synthesis

In the previous *Chapter 3.2.2.3*, the most common methods of synthesis of graphite oxide are summarized. The graphite oxide prepared by Staudenmaier method has a relatively regular structure, and its oxidation degree can be controlled by the oxidation time, but it is prone to explosion in the reaction process thus has a high risk. The Brodie method takes less time to prepare graphite oxide, has a higher degree of oxidation, and is relatively safer than other methods. At present, Hummers method is the most common method for preparing graphite oxide, and has been modified by many researchers in literatures. ***Modified Hummers method was used to prepare Graphite Oxide in this paper.*** In the previous *Chapter 3.2.2.4*, the exfoliation methods of Graphite Oxide to Graphene Oxide are listed and among them the ultrasonic exfoliation is fully explained, which is adopted during the experiment of this paper. Freeze drying technique mentioned in the *Chapter 3.2.2.5* is used to dry excess solvent to obtain dry graphene oxide powder. The specific experimental procedures used in this paper are as follows:

40 mL of H_2SO_4 was placed in a large beaker, ***cooled in an ice bath (important for safety)***, followed by the addition of 2g of *Graphite flake* (Natural, 325 mesh) and 1g of $NaNO_3$. The mixture was stirred for 15 min below 5 ℃ after which 15g of $KMnO_4$ was ***added slowly*** within 10 min. After 30 min at around 10 ℃, the reaction was continued for 60 min at room temperature. Then 90 mL of deionized water was dropped into the mixture and the temperature of reactants

rose to around 95 ℃. The viscous mud was diluted in 500 ml of water and the unreacted $KMnO_4$ was reduced with 30% H_2O_2 until the slurry turned dark brown.

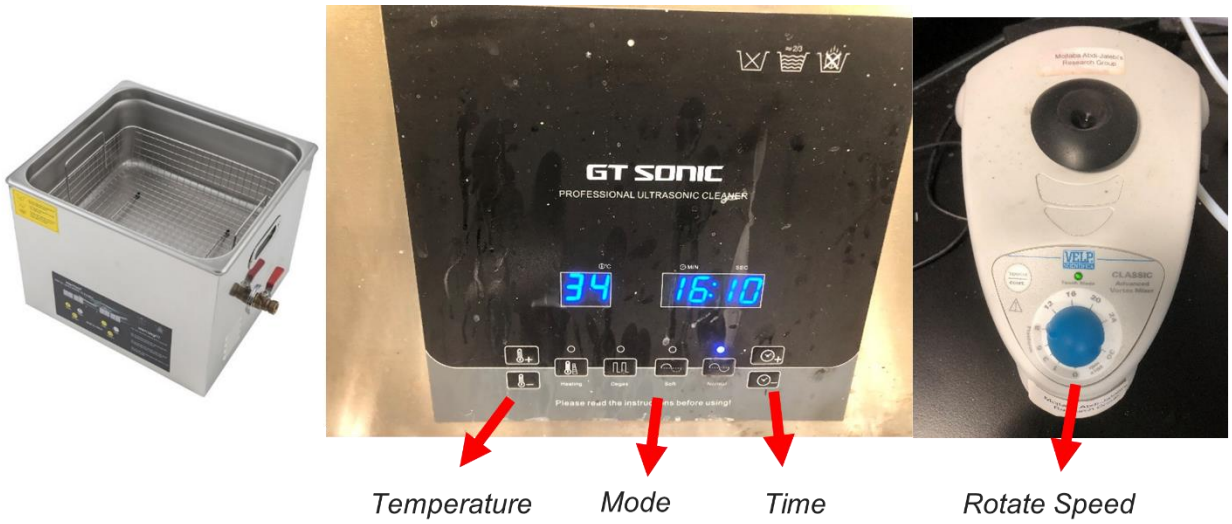


Figure 10 (a b c from left to right): (a) Typical laboratory ultrasonic cleaner.

(b) Operation interface of ultrasonic cleaner.

(c) Vortex mixer.



Figure 11 (a b c from left to right): (a) Vacuum freeze drying instrument.
(b) Weighing Scale. (c) Deionizer.

The product was ultrasonic treated, centrifuged, washed with dilute hydrochloric acid and hot water, and finally wet graphene oxide was obtained, shown as yellow-brown viscous mud in *Figure 12(a)*. Then use freeze drying technique to get dry graphene oxide powder. 1-2ml graphene oxide deionized water was added in a small glass bottle. Five sealed bottles with samples were put in the freezer for 3 days until the water was totally frozen. Then holes are made on the seal tape to extract water. 20mg dark-golden-yellow graphene oxide was obtained following the above procedures. The instruments used during the experiment are shown in the *Figure 11*. The products obtained during the experiment are shown in the *Figure 12* in order.

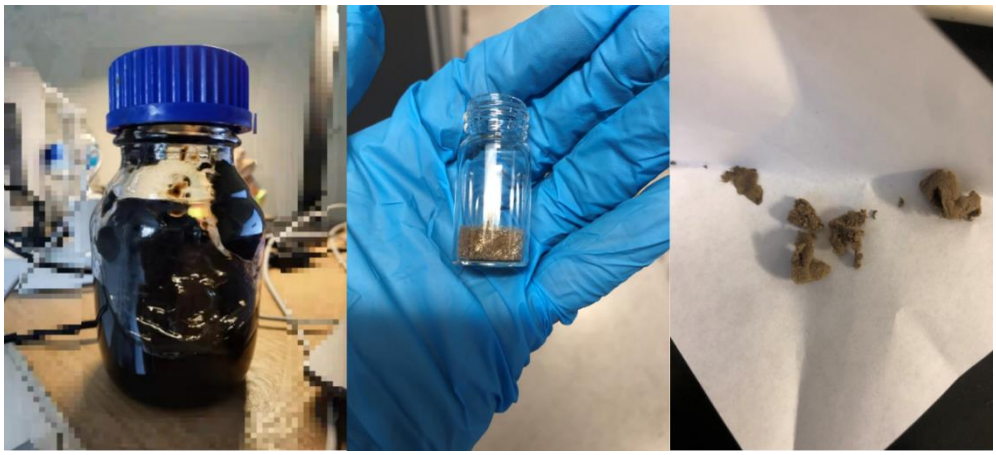


Figure 12 (a b c from left to right): (a) Wet GO.
(b) Dry GO powder just after freeze drying. (c) Dry GO product.

After experiment, GO was dispersed in Water, Isopropanol, Acetone respectively to test its solubility. Ultrasonic treatment and vortex mixing (Shown in *Figure 10*) was further used to exfoliate probably residual graphite oxide during the dissolution. As can be seen from *Figure 13*, GO produced by Hummer's method obtains good dispersion in water and isopropanol (polar solvent). The good dispersion of GO in water and polar solvent mentioned in *Chapter 3.2.1* was proved. And few precipitations can be observed when dispersed in Acetone, which was considered as lower solubility. Therefore, supernatant of Acetone/GO solution should be taken for further procedures if needed.

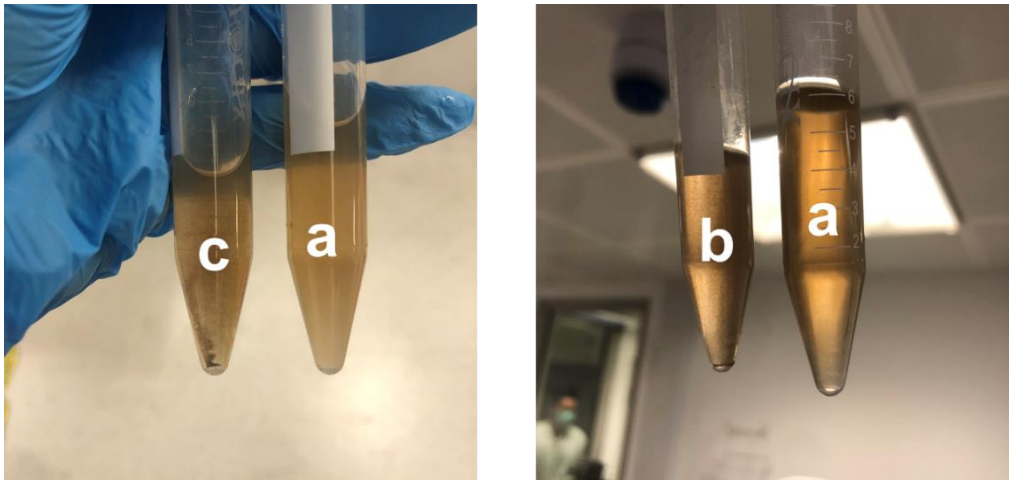


Figure 13 (a) GO dispersed in Water.
(b) GO dispersed in Isopropanol. (c) GO dispersed in Acetone.

3.2.3 Characteristics, Properties and Synthesis of reduced Graphene Oxide

Both graphite oxide and graphene oxide are insulating materials due to their SP^2 cellular structures. However, both graphite oxide and graphene oxide can become conductive materials again by connecting their conjugated network, therefore the reduction of GO is one

of the most important reactions of GO. Due to the wide application of graphene, reduction of GO is the most suitable method for large scale preparation of graphene materials. The reduction of GO is mainly achieved by chemical reduction, thermal reduction and electrochemical reduction [90]. Among them, Go can be a precursor of graphene by chemical or thermal reduction, the relationship between graphene, graphene oxide and reduced graphene oxide can be briefly summarized in *Figure 14*.

Thermal reduction means that graphite oxide is heated rapidly in high temperature. Because the surface of graphite oxide is rich in a large number of oxygen-containing groups such as hydroxyl and epoxy groups, these oxygen-containing groups will detach from the graphite sheet in the form of small molecules such as carbon dioxide or water molecules at high temperature. Because graphite oxide is heated rapidly at high temperatures, the rate of gas formation will be greater than the rate of its release. At this point, the pressure between the layers due to the lack of time for the gas to be released from the system may be greater than the van der Waals forces that bind the graphite, thus freeing the graphene sheets from the van der Waals forces.

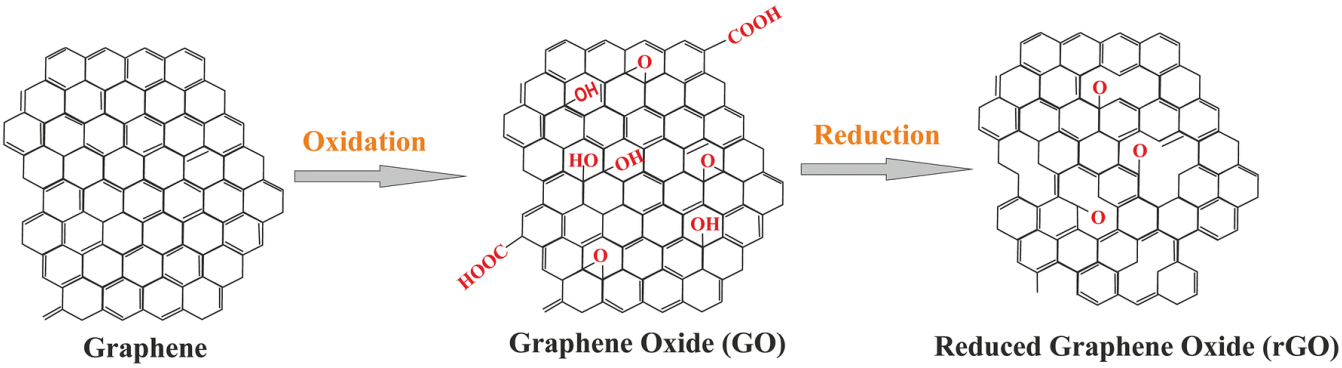


Figure 14: The relationship between Graphene, GO and rGO.

For chemical reduction, a number of chemical reagents can be used to reduce GO when it is dispersed in a solvent as a colloid. However, the first substance reported to be used to reduce GO is hydrazine hydrates. Although most strong reducing agents have a slight tendency to react with water in water except hydrazine. This property of hydrazine makes it the preferred candidate for reducing go dispersed in water. In 2006, Stankovich and Ruff et al [91] from North-western University of America reported in Nature that graphene sheets with thickness can be prepared by REDOX method to form polystyrene nanocomposites. When the GO is reacting with the Hydrazine, the GO will no longer disperse in water, but instead will form black precipitations. This phenomenon is caused by the reduction of the polar functional groups on the GO sheet after the reaction, resulting in a decrease in the hydrophobicity of GO.

In addition, other reducing agents have also been used in recent studies. Sodium hydrogen boride ($NaBH_4$) is considered to be a better reductant of GO than Hydrazine [92]. Although its

hydrolysis in water is slow, enough time is given by this for the formation of sufficient reducing agents to reduce GO. The electrochemical reduction of GO mainly depends on the electrochemical movement of oxygen-containing functional groups on GO. It can avoid the use of dangerous reducing agents and the steps of disposing of by-products, but its principles are still being explored and no representative method has emerged nowadays.

Although three GO reduction methods have been mentioned previously, none of the reported reduction methods can completely remove oxygen groups and only achieve partial recovery of the graphene network. This can also be seen clearly in the *Figure 14*. In addition, there are many defects in the rGO substrate. As carbon evolves in the form of CO or CO_2, the thermal reduction process results in holes in the base plane. Chemical reduction of reductants also results in the formation of defects and layered structures on the rGO surface and may lead to additional doping of the defect site. Due to these reasons, in the experiment of this paper, rGO is directly supplied from ALDRICH for its low price and easy operation, shown in the *Figure 15* below.



Figure 15 (a b c from left to right): (a) Reduced Graphene Oxide.
(b) Well dispersed rGO/EP solution
(c) Probe Ultrasonic instrument.

3.3 Graphene / Polymer Nanocomposite

3.3.1 Introduction of Epoxy Resin

Among all kinds of resins, epoxy resin (EP) is a kind of commonly used thermosetting resin, and is widely used in polymer matrix composites. EP is a thermosetting polymer used in a wide variety of industries such as coatings, adhesives, laminates, electrical insulators, industrial and composite applications. Epoxy resin has excellent mechanical and chemical properties, including good dielectric properties, high dimensional stability, hardness, flexibility and

excellent chemical stability [93-97]. Epoxy resin is obtained from polycondensation reactions between epichlorohydrin and bisphenol/polyol/polyacid/polyamine, and its molecules contain two or more epoxy groups. In addition, epoxy resin has the characteristics of low shrinkage, low cost and easy processing and forming, and has a wide range of applications in machinery, chemical industry and aerospace fields. The disadvantage of epoxy resin lies in its high internal stress and poor impact resistance after curing, which limits its application to a certain extent.

The molecular chain of epoxy resin contains active epoxy groups. The epoxy group is a ternary ring composed of two carbon atoms and one oxygen atom, all three atoms in a plane. In the epoxy group, the electronegativity of oxygen is greater than that of carbon, resulting in "electrostatic polarization" as well as a larger density of electron clouds around oxygen atoms and a smaller density of electron clouds around carbon atoms [98]. Therefore, in the epoxy group there are two reactive center oxygen atoms with a high electron cloud density and carbon atoms with a low electron cloud density. In the reaction, the $C-O$ bond breaks, resulting in ring opening of the epoxy group [99]. Because of the polarization of charge and the large deformation energy of epoxy group, it has high reactivity. The reactivity of epoxy group enables ring-opening polymerization to react with a variety of compounds containing active hydrogen. For example, reactions between epoxy group and primary amine, secondary amine or other amine, alcohol, as well as phenol and hydroxyl acid, which all gift epoxy resin with high reactivity.

Epoxy resin itself has a thermoplastic linear structure. Crosslinking curing reaction will work only after adding curing agent, under certain conditions [100]. So that a network structure is formed and applicable. During the curing process of epoxy resin, the epoxide group and hydroxyl group in its molecule are the active centers, which can react with many active functional groups. During the curing of epoxy resin, the internal factors affecting the curing reaction are the structure of epoxy resin and curing agent, while the curing temperature, the content of carbon dioxide in the air and solvent are external conditions. During the curing reaction process, the internal factors and external conditions work together to change the curing reaction process of epoxy resin. Curing agent is an important part of the curing system of epoxy resin. As a kind of additive, the curing agent reacts with epoxy resin chemically, forming a network of three-dimensional polymer, so that the linear structure of epoxy resin gets into a tough stereochemical structure.

For the experiment of this paper, epoxy resin was supplied by DELO. The type is DELO KATIOBOND LP655, its technical datasheet is attached as *Appendix 1*. It is a kind of modified epoxy resin which is free of solvents, thixotropic and tested to be able to provide high water vapor barrier. Compared with other types of epoxy resin, its operation is much more convenient since it does not need curing agent to perform cross linking curing reaction. And because it is

free of solvents, UV- / Vis-curing can be directly used after simple coating as long as its uniformity is achieved. The suitable lamp types can be LED 365nm, LED 400nm and UVA and its typical irradiation time only needs 20s under the condition of $200mW/cm^2$ intensity, which is easy to operate and suitable for bulk production considering its relatively low price.

In many studies, epoxy resin based nanocomposite is used to improve its thermal behaviour, including thermal stability and flame retardancy [100]. However, considering other good properties of epoxy resin including good dielectric properties, high dimensional stability, hardness, flexibility and excellent chemical stability, it can adequately be used for the encapsulation application of graphene/polymer nanocomposites. None of the studies has suggested this possibility so far. Although the mechanisms are different, it can be considered to share the same basic idea as organic/inorganic multilayer encapsulation method, which is mentioned in *Chapter 2.2.3*. The epoxy resin in the nanocomposites can be regarded as organic layer, plays a role in improving the sample surface flatness and reducing mechanical loss while graphene and its derivatives provide the function of gas barrier. Actually, the epoxy resin used in this paper was able to provide extra high water vapor barrier, as shown in the product specification of Appendix 1. In general, graphene and its derivatives are incorporated into polymer matrix mainly to enhance mechanical strength, improve electrical conductivity, and give gas barrier properties. In addition, different types of polymer matrix and different types of graphene fillers can be selected according to the application of nanocomposites. Therefore, there are good reasons to believe that the nanocomposites of GO/rGO and EP is expected to have good mechanical strength, flexibility, dielectric properties, high stability, optical transmittance and superior gas barrier performance, which are the essential properties of a good OLED encapsulation method.

3.3.2 Synthesis of Graphene/Polymer Nanocomposites

As for the preparation methods of Graphene/polymer nanocomposites, there are mainly three methods: Melt processing, In situ polymerization and solution mixing method [101].

The preparation of thermoplastic polymer nanocomposites by melting is a typical method. It is an environmentally friendly, inexpensive, suitable for large-scale production of industrial applications [102]. The polymers are heated until they are in a molten state, and then the mechanically mixed molten compound is extruded. Solvents are not required in the smelting process, but in the process, strong shear forces are required to mix the highly viscous molten polymers with graphene derivatives. Here, graphene buckling may occur, leading to rolling or shortening of graphene derivatives.

In situ polymerization is another method for the preparation of uniformly dispersed graphene or GO nanosheets in a polymer matrix because of the interaction between graphene

derivatives and the polymer matrix to form chemical bonds. In addition, by inducing additional functional groups on graphene or go surfaces, in situ polymerization can enhance the dispersion properties and improve graphene compatibility with polymers through chemical bonding [103]. Fine powder or uniformly dispersed graphene nanosheets in a solvent can be mixed with a monomer solution containing a photo initiator or a thermal initiator. After the initiator is dissociated by radiation or thermal energy, the stripped graphene or GO nanosheets can be mixed or crosslinked with the polymer chain and this results in higher dispersion characteristics. However, viscosity usually increases during polymerization, which may reduce the machinability of nanocomposites.

The solution mixing method is widely used because of its simplicity. The key challenge in solution mixing is to minimize residual solvents and obtain good dispersion of fillers in viscous polymer solutions. Complete drying is required to eliminate residual solvents. In the case of go as nanofillers, thermal reduction of GO should be carefully considered, as go readily degrades even at low temperatures around $150\,^{\circ}C$ [104]. This usually results in local structural deformation of the polymer matrix, which results in a significant loss of the physical properties of the resulting graphene/polymer nanocomposites. Therefore, the solution mixing method has an advantage in this regard. The composition of graphene nanosheets is significantly affected by the degree of dispersion in the mixed solution. In addition, aggregated graphene or GO nanosheets are a key problem that often arises in such nanocomposites due to poor solubility or gravimetric precipitation of unshed graphene or GO nanosheets. Therefore, the choice of solvent is very important in solution mixing.

3.3.3 Practical Experimental Method of GO/EP and rGO/EP Synthesis

As mentioned in the previous chapter, considering the thermal reduction of GO, solution mixing is a convenient and safe method if the right solvent can be selected to achieve good dispersion and complete elimination of residual solvents.

For rGO/EP nanocomposite, 25mg rGO was dispersed in 25ml Ethylene Glycol (EG) with ultrasonic treatment $(40℃)$ for 1hour firstly. 10ml supernatant of solution is mixed with 10ml Acetone for the dispersion of EP with stirring and vortex mixing for 1hour. Then 2ml EP was added to the solution with ultrasonic treatment for 1hour. After these procedures, the well dispersed rGO/EP solution is obtained, without obvious solid precipitation after 1 week, which is shown in the *Figure 15 (b)*. Ethylene Glycol and acetone can be mutual dissolved, which is essential to both good dispersion of rGO and EP.

For GO/EP, many researchers [100,105] choose to use Acetone as the solvent for both GO and EP. However, as mentioned before, the GO synthesized in the experiment shows low solubility in Acetone even after high power probe ultrasonic treatment, which is shown in the *Figure 13*

(c). Therefore, by looking up other researcher's experience on Internet forums and getting suggestions from my supervisor Dr. Mingqing Wang, other types of solvents such as Ethylene Glycol, Ethyl Alcohol and Isopropanol are used respectively. *Figure 16* shows the GO/EP solution obtained from the use of Acetone, Isopropanol and Ethylene Glycol respectively. As can be seen from the *Figure 16 (a)*, there are obvious precipitations in the GO/EP solution obtained from Acetone. In *Figure 16 (b)*, GO and EP dispersed well in Isopropanol at the beginning, however, the solution gradually became opaque, which was not observed in the GO/Isopropanol Solution in *Figure 13 (b)*. Thus, this is supposed to be epoxy resin agglomerating in solution. As shown in *Figure 16 (c)*, well dispersed GO/EP solution was obtained by the use of Ethylene Glycol. The specific procedures are as follows:

First, 1.5mg GO was dispersed in 45ml Ethyl Glycol with Probe Ultrasonic treatment for 1hour. 10ml Acetone and 1ml EP were consecutively added to the solution with ultrasonic for 1h and stirring for 0.5hour, vortex mixing for 0.5hour. After these procedures, the well dispersed GO/EP solution is obtained, without obvious solids precipitation after 1 week's quiescence.

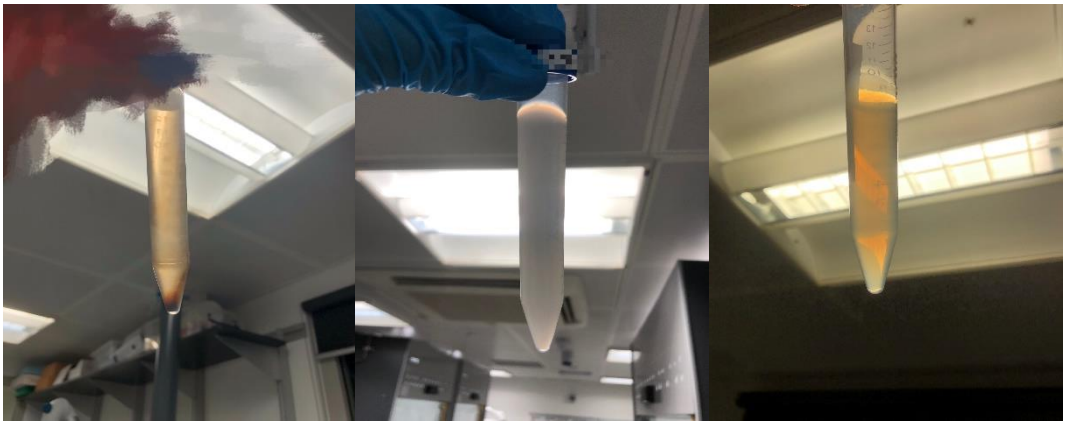


Figure 16 (a b c from left to right): (a) GO and EP dispersed in Acetone.
(b) GO and EP dispersed in Isopropanol.
(c) Well dispersed GO/EP in Ethyl Glycol.

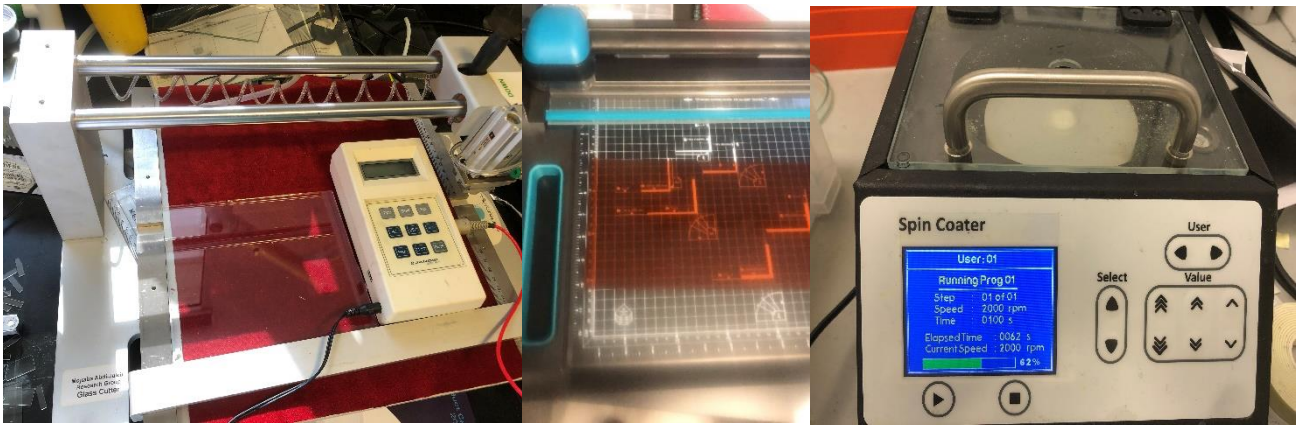


Figure 17 (a b c from left to right): (a) Cutting instrument for glass substrates.
(b) Cutting instrument for flexible substrates. (c) Spin coater.

3.4 Preparation of Samples for Characterization

After the preparation of well dispersed GO/EP and rGO/EP solution, it is accessible to prepare thin films on different types of substrates. Glass substrates and flexible substrates were prepared respectively. For cutting process, instruments used for glass substrates (2.5cm*2.5cm) and flexible substrates (5cm*5cm) are shown in the *Figure 17*. After cutting, the substrates were dipped in deionized water with 5 minutes' ultrasonic treatment for cleaning. Then moderate amount of acetone was taken for further cleaning, followed by drying process using pressured nitrogen blowing concentrator. The films can be coated on the substrates using different methods, the common ones include dip coating, vacuum filtration and spin coating. Among them, dip coating often results in heterogeneous deposition, resulting from self-aggregation [34]. The vacuum filtration has been suitable and by adjusting the amount of the filtered GO suspension, different nanoscale thickness of films can be achieved. However, it is relatively complex and time consuming. Spin coating can not only prepare uniform films but also simple and fast. The thickness of the film can also be controlled by adjusting the rotating speed and duration, or the amount of dripped solution. The spin coater used during experiment is shown as *Figure 17 (c)*.

GO/EP, rGO/EP solution were separately dripped onto 3 glass substrates and 2 flexible substrates. Different rotating speed, duration time and amount of dripped solution were tested, the best combination of set was adopted. For GO/EP, 3000/2500/2000/1500 rpm for 60 seconds were set and coated. For rGO/EP, 5000/4000/3000/2000 rpm for 60 seconds were set and coated. All the coated substrates were firstly heated at 80 ℃ on a hot plate for 30min to eliminate the residual solvent and then cured under ultraviolet light (UV) for 30s. The used instruments are shown in the *Figure 18*. In the following section of this paper, we use abbreviations for these samples. For example, GO 3000 is short for GO/EP nanocomposites film under the condition of 3000 rpm and 60 seconds for spin coating.



Figure 18 (a b c from left to right): (a) Hot plate. (b) UV light. (c) Dark room for curing.

4. Results and Discussions

4.1 Film Thickness Measurement

BRUKER DektakXT Profiler is used to measure the thickness of films, shown in the *Figure 20*. Step meter belongs to contact surface topography measuring instrument. The measuring principle is that when the probe slides gently along the measured surface, the probe moves up and down along the peak and valley while sliding because of the tiny peaks and valleys on the surface. The motion of the probe reflects the contour of the surface. After measuring the electric signal output by the sensor, the output amplitude modulation signal is proportional to the displacement of the probe deviating from the balance position. After amplification and phase-sensitive rectification, the displacement signal can be demodulated from the amplitude-modulated signal to obtain the amplified signal which is proportional to the displacement of the probe. Then noise filter and waviness filter are used to filter the influence of modulation frequency, external interference signal and waviness on roughness measurement [106].

rGO 2000, rGO 3000, rGO 4000, GO 2000 totally 4 samples are measured. It is noticeable that a part of film should be scrapped before measuring so that the difference between values of Y-axis at initial range and back range of X-axis. This can be explained clearly using the software diagram.

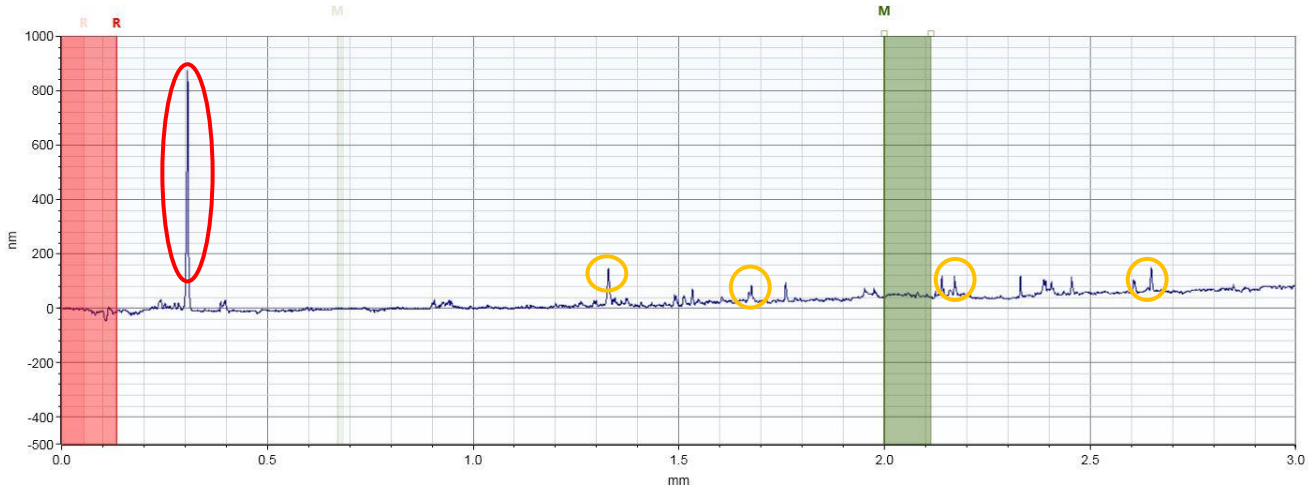


Figure 19: Profiler diagram of GO 2000.

The *Figure 19* above shows a profiler diagram of GO 2000, the X-axis represents the distance the probe has travelled and Y-axis represents the displacement of probe in vertical direction. An initial range of X-axis is selected, shown as red zone in the diagram. And the selected green range represents back range of X-axis. There exists difference because of the scrapped part. To be noticed, relatively smooth part of curve should be chosen rather than those parts with yellow and red circles, which are shown in the *Figure 19*. And to ensure the accuracy of average value, it is better for the width of range to be greater than 1mm. The red circled part

is supposed to be dust created during scrapping. The yellow circled part is supposed to be uniform part of the film, which may be caused by the coating or heating process during preparation. Apart from that, the overall film is fairly uniform.

With diagrams like this, we can calculate the thickness of the film. The films thickness of 4 samples are listed in the *Table 2* below. It can be seen from *Table 2* that as rotating speed increases, the thickness of the film decreases, and there is an approximate linear relationship between them. Every 1000 rpm increases will result in an approximate decrease of 5nm. Although more experiments are supposed to be conducted to prove this relationship, the realization of controlling film thickness by adjustment of rotating speed during spin coating in nanoscale, mentioned in *Chapter 3.4*, is achieved.

	GO 2000	*rGO 2000*	*rGO 3000*	*rGO 4000*
Position (mm)				
R	*0.1336*	*0.4914*	*0.3911*	*0.2776*
M	*1.9993*	*3.3891*	*2.1748*	*2.1306*
Δ	*1.8657*	*2.8977*	*1.7837*	*1.8530*
Width (mm)				
R	*0.1336*	*-0.4475*	*0.3657*	*0.4169*
M	*0.1138*	*-0.5062*	*0.3987*	*0.4092*
Total Profile (nm)				
R	*-15.9207*	*4.5525*	*5.1443*	*-7.2993*
M	*39.7905*	*46.9613*	*42.4558*	*25.1144*
Δ_T	*55.4113*	*42.4089*	*37.3125*	*32.4138*

Table 2: R represents the selected red zone.

M represents the selected green zone. Δ_T indicates the thickness.



Figure 20: (L) Profiler. (R) Contact Angle instrument.

4.2 Contact Angle Measurement

The contact angle (θ) refers to the angle between solid-liquid interface and gas-liquid interface at the junction of solid, liquid and gas. The contact angle of liquid on the surface of solid material is an important parameter to measure the wettability of liquid on the surface of material. A lot of information about solid-liquid and solid-gas interface interactions can be obtained by measuring the contact angle. If θ<90°, the solid surface is hydrophilic, that is, the liquid is easier to wet the solid, the smaller the angle, the better the wettability. If θ>90°, the solid surface is hydrophobic, that is, the liquid does not moisten the solid easily and moves on the surface easily. This kind of wetting process is closely related to the interfacial tension of the system. A drop of liquid falls on a horizontal solid surface, and when equilibrium is reached, the contact angle formed between the surface tension and the contact angle conforms to Young's formula below:

$$\gamma SV = \gamma SL + \gamma LV \times cos\theta e$$

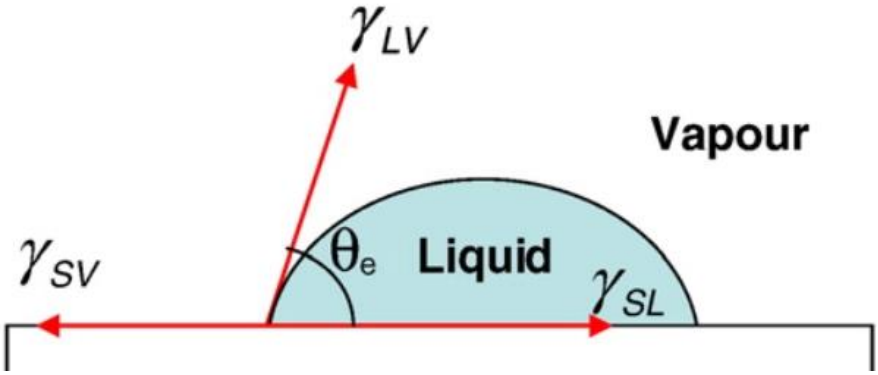


Figure 21: Schematic diagram of contact angle.

The principle of contour image analysis is to drop droplets on the surface of solid samples, obtain contour images of droplets through microscopic lens and camera, and then use digital image processing and some algorithms to calculate the contact angle of droplets in the image. In the experiment, the droplets were dropped at GO 3000, GO 1500; rGO 5000, rGO 2000 samples respectively to test hydrophilicity. The instrument used is shown below in *Figure 22*.

The results are shown below in the *Figure 22*. As can be seen that the contact angle of GO is far smaller than rGO, $87.06°$ of GO 3000 compared to $123.58°$ of rGO 5000 and $93.59°$ of GO 1500 compared to $120.89°$ of rGO 2000, which indicates the rGO/EP film has a better hydrophobicity than GO/EP. It is noticeable that despite the thickness of GO and rGO film changes, there is only subtle difference, $93.59°$ to $87.06°$ and $120.89°$ to $123.58°$ There is no obvious relationship between film thickness and contact angle. Although the hydrophilia is an important property of the film evaluating the encapsulation performance, the basic barrier mechanism of graphene is not the interfacial tension, as mentioned in *Chapter* 3.1.3. Therefore,

a good hydrophobicity does not necessarily mean that the film can provide good gas barrier and the reverse is also true.

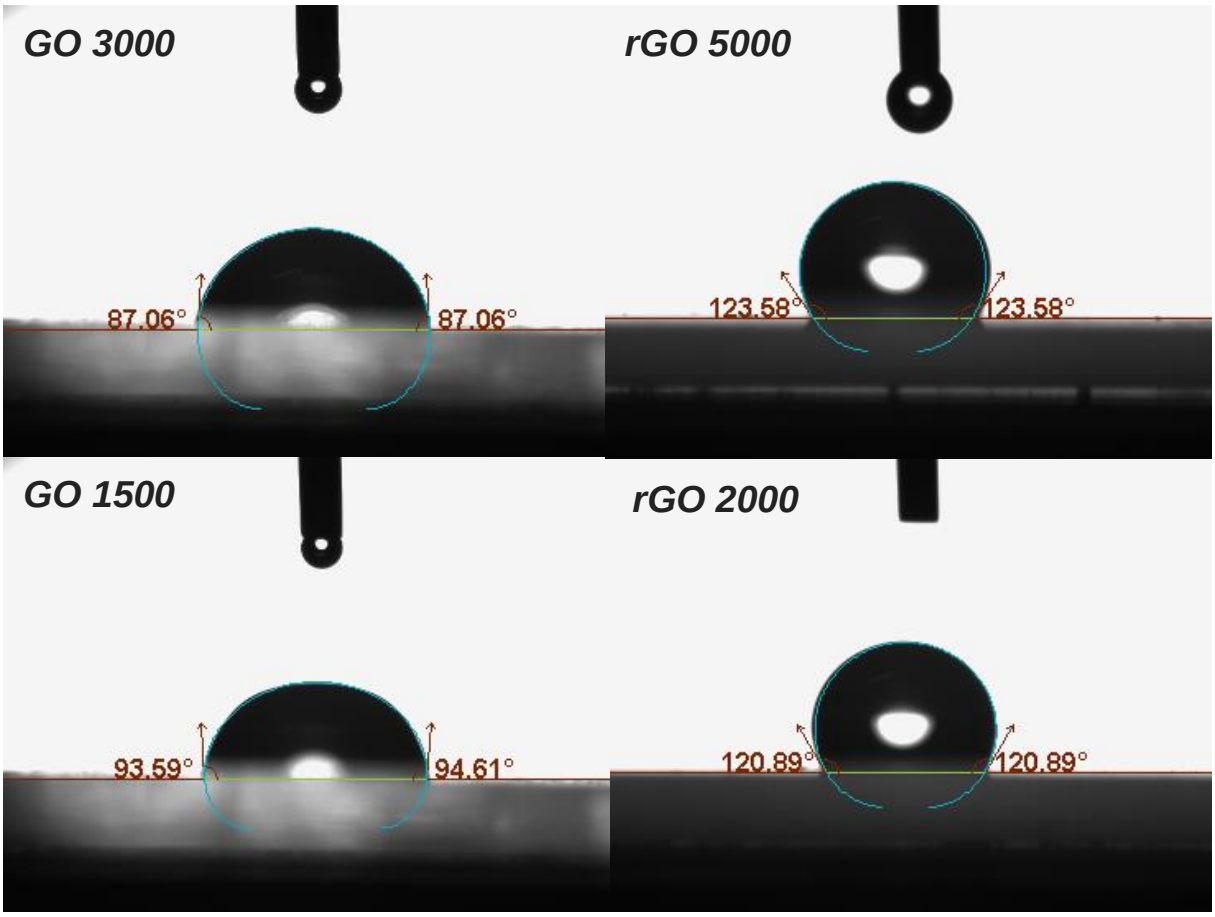


Figure 22: Contact angle measurement of 4 samples, rGO 5000/rGO 2000/GO 3000/GO 1500.

4.3 Transmittance Measurement

Transmittance is an important parameter for OLED encapsulation in terms of light emitting, as mentioned in *Chapter 2.1.1 and 2.2.3*. Transmittance indicates the ability of light to pass through a medium. It is the percentage of the light flux passing through a transparent or semi-transparent body compared to the light flux entering it. It is assumed that when parallel monochromatic light passes through a uniform, unscattered medium, part of the light is absorbed, part of the light passes through the medium, and part of the light is reflected by the surface of the medium. Transmittance can indicate the efficiency of light transmission of display equipment, which directly affects the visual effect of touch screen. The value T of transmittance is a percentage, ranging from 0 to 100%. If all the light is absorbed by the medium, T=0. If the light is completely transparent, T=100%.

Spectrometer is a scientific instrument that decompose complex light into spectral lines. It is composed of prism or diffraction grating, etc. Spectrometer can measure the light reflected from the surface of objects. PerkinElmer Lambda 750S UV/VIS/NIR Spectrometer was used

and the chamber of the instrument is shown below as *Figure 24 (a)*. 6 samples: rGO 2000, rGO 3000, rGO 4000; GO 1500, GO 2000, GO 2500 are tested and the results are shown in *Figure 23*. The glass substrate without film was measured first to reduce its influence on results. It is noticeable that the data exported by software sometimes show as absorbance, represented by A:

$$A = \lg\left(\frac{1}{T}\right) \quad (9)$$

As can be seen from the Figure 23, although rGO/EP films have a generally good transmittance, larger than 96.5%, which is adequate for OLED application, GO/EP films perform better, mostly larger than 97.5%. The high transparency of graphene gifts nanocomposites films with this excellent property, fulfilling the application requirements. It is worth noting that as the rotating speed increases, transmittance of both GO/EP and rGO/EP films increases as well. This may be because the larger thickness will result in the reduction of transmittance.

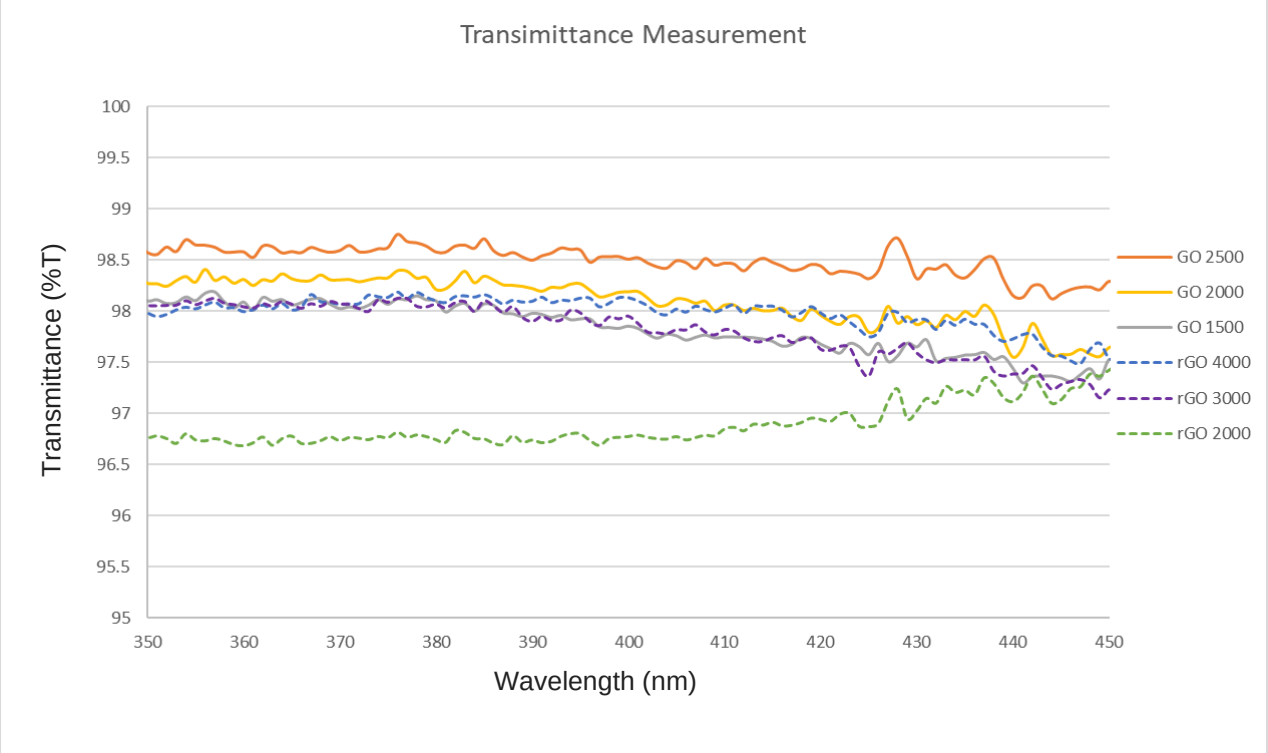


Figure 23：Transmittance diagrams of 6 samples,

GO 2500/GO 2000/GO 1500/ rGO 4000/rGO 3000/rGO 20000

4.4 X-ray Diffraction Patterns

X-ray Diffraction Patterns (XRD) is a testing method for phase analysis and identification using diffraction phenomena generated when rays are projected onto crystals. It can be used to measure the crystal plane spacing, cell size and type of the phase, etc. X'Pert PRO is the instrument used, shown in the *Figure 24*. Natural Graphite, GO and rGO are respectively coated on glass substrates and then measured.



Figure 24 (a b c from left to right): (a) The chamber of UV spectrometer.

(b) The XRD test platform. (c) XRD instrument.

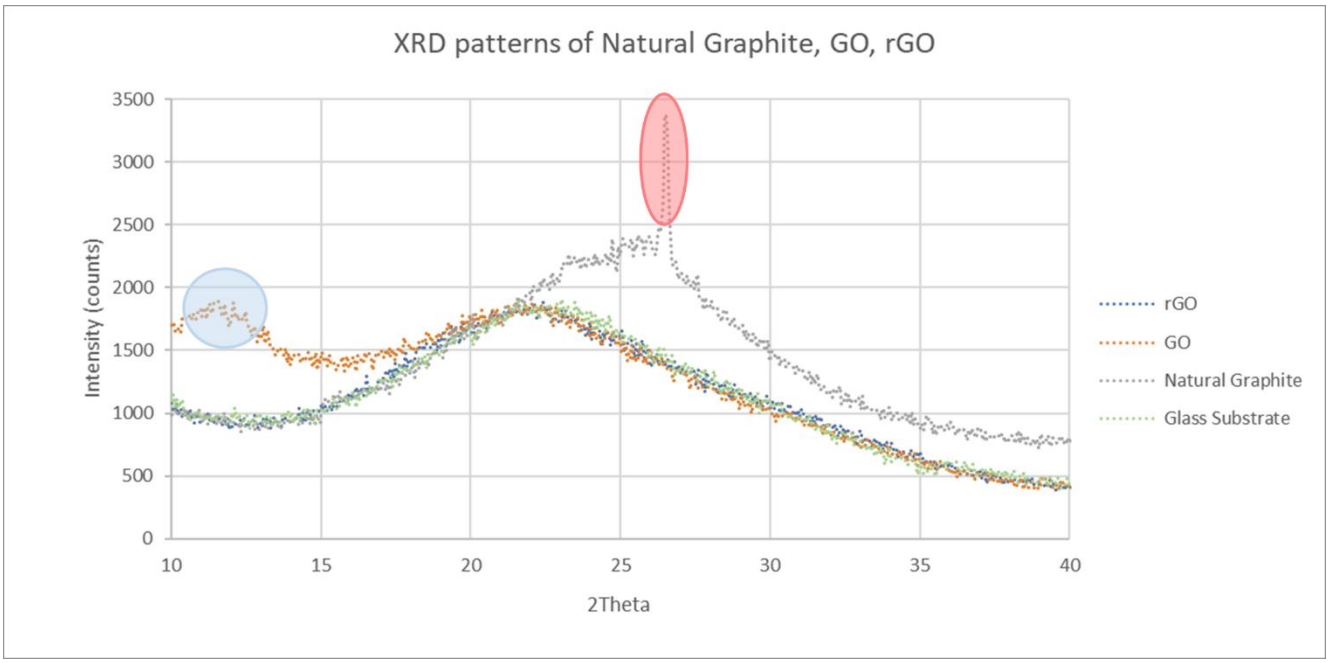


Figure 25: XRD patterns of Natural Graphite, GO and rGO. (Not Relative Intensity)

As can be seen from the XRD patterns of Natural Graphite, GO and rGO in *Figure 25*. There is a strong peak at $26.5°$ for Natural Graphite pattern, which is supposed to be the 001 diffraction peak of the natural graphite crystal plane, corresponding to the highly regular crystal structure of natural graphite. According to Bragg equation:

$$2dsin\theta = n\lambda \quad (10)$$

Where,

$$n = 1$$

$$\lambda = 1.54\text{Å}$$

The interlayer spacing of natural graphite is calculated to be 0.34nm, which is highly consistent with the literature [107].

For the pattern of GO, the peak at $26.5°$ disappears and instead a broad peak at $12.3°$. The interlayer spacing of GO is calculated by *equation (10)* to be 0.72nm. This is due to the insertion of hydroxyl and carboxyl groups in the oxidation process. This result is in good agreement with

the crystal plane spacing reported in the literature [108]. This result confirms that the Modified Hummers method does lead to complete oxidation of graphite. It is worth noting that for the pattern of rGO, it almost coincides with the pattern of glass substrate without any peak. The reason for this phenomenon is that rGO has been completely stripped after reduction, so there is no longer diffraction peak of crystal plane in the spectrogram, showing disorder and exfoliation.

4.5 FTIR Spectrum of Graphene Oxide

The functional groups in graphite oxide can be determined by FTIR spectroscopy. The instrument used is shown in *Figure 27*. The FTIR spectra of Graphene Oxide is shown in *Figure 26*. In the X-H stretching vibration zone, there is a wide and strong absorption peak 3402. It corresponds to the stretching vibration of O-H, which is the vibration of adsorbed -OH in the water. The band between 2875 and 2938 corresponds to C-H stretching vibrations. In the double bond stretching vibration region, absorption peak 1724 is assigned to the stretching vibration of C=O bond in hydroxyl or carboxyl functional groups. Peak 1401 corresponds to the stretching vibration of the C-O bond in the carboxyl group. Peak 1273 is due to the O=P group and the new band 1036-1060 corresponds to -P-O-C group, which is derived from functionality of phosphorus [100]. The *Figure 26* also shows some small peaks corresponding to embedded acids and oxidants. According to the above analysis, it is shown clearly that there are a large number of oxygen-containing functional groups in graphene oxide mainly including -OH, -COOH and C-O-C as well as a certain number of C=C, C=O, O=P bonds.

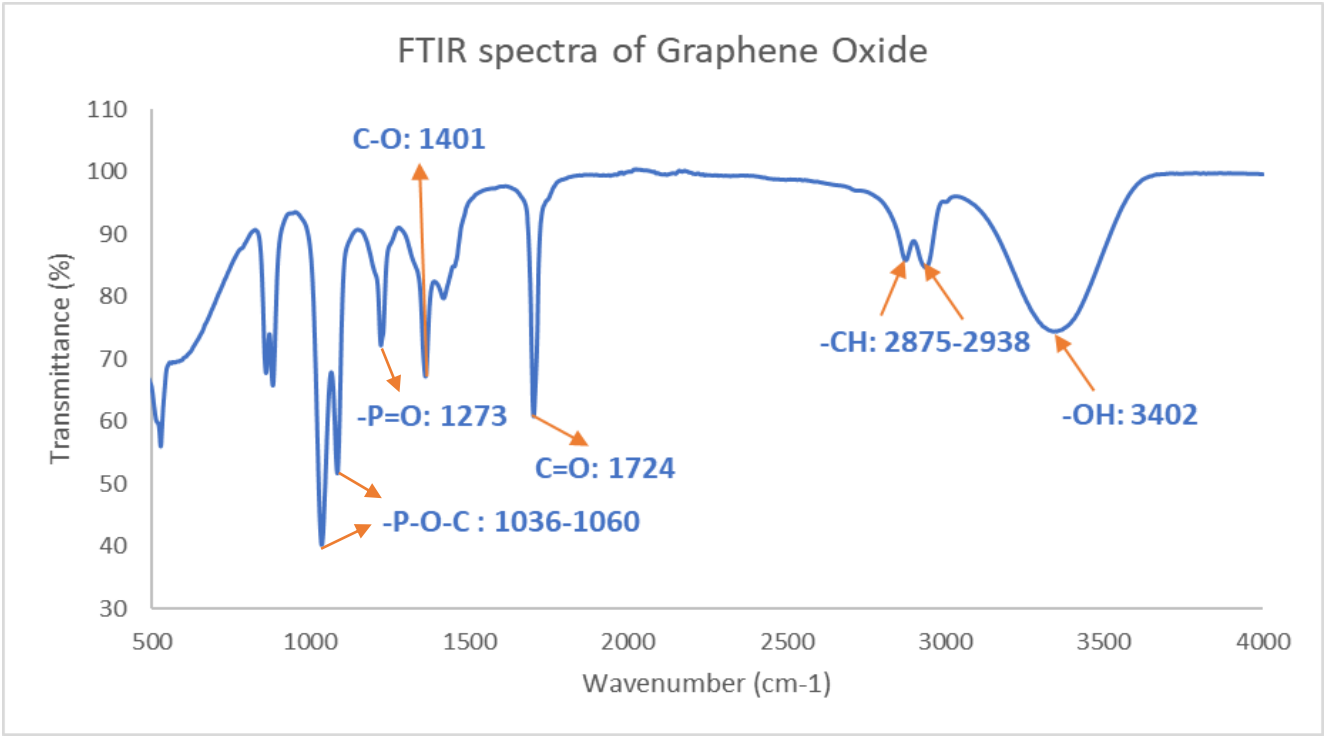


Figure 26: FTIR spectra of Graphene Oxide

4.6 SEM Analysis

Scanning electron microscope (SEM) is a large precision instrument used for high resolution microtopography analysis. It has the characteristics of large depth of field, high resolution, intuitive imaging, strong three-dimensional sense, wide magnification range, and the sample to be tested can be rotated and tilted in three-dimensional space. In addition, it has the advantages of abundant samples, almost no damage and pollution of the original sample, and can obtain morphology, structure, composition, and crystallography information at the same time. Despite good electrical conductivity of Graphene, the conductivity of GO/EP or rGO/EP film is not clear, therefore surface gilding is necessary. Quorum Q160R is used to glid the film surface, and HITACHI TM4000Plus is used for observation and taking photos.



Figure 27: (Left-Up) FTIR instrument. (Left-Down) Surface gilding instrument. (Right) Scanning electron microscope.

From *Figure 28 (a) and (b)*, obvious scaly structures of rGO and GO are observed, shown as bright spots with 5k magnification. The surfaces of both are distributed with some flaps, which are rGO and GO sheets with nonuniformity. *Figure 28 (b)* has a less uniform surface than (a) and the layers in structure are relatively loose. The lamellar structure of GO is smaller because during the process of oxidation, the strong acidity of concentrated sulfuric acid destroys the graphite sheets. The surface of pure epoxy resin is very flat and dense shown as *Figure 28 (c)*. After incorporation of GO into polymer matrix and adjustment of adding magnification to12k, a uniform and free of any impurities nanocomposite film is shown as *Figure 28 (d)*. There are reasons to believe that the film has superior gas barrier performance and can be applied to encapsulation of OLED.

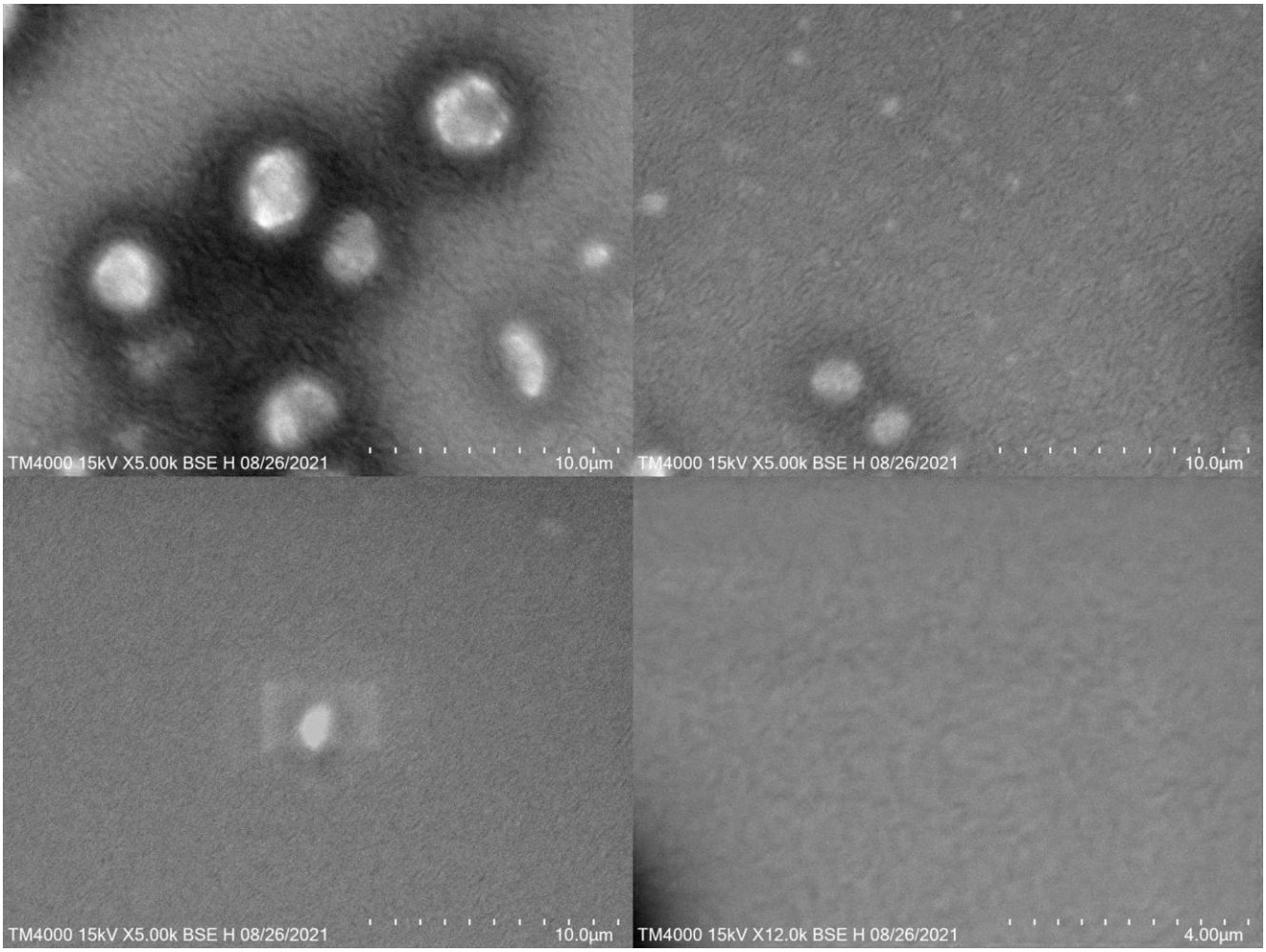


Figure 28: SEM images of (Left-Up-a) rGO. (Right-Up-b) GO.
(Left-Down-c) Pure Epoxy Resin (Right-Down-d) GO 2000 film on glass substrate.

5. Conclusions and Outlook

In this paper, a comprehensive review of development in encapsulation methods of OLED is delivered first. Application of graphene and its derivatives in barrier polymer is then introduced and the characteristics, properties and synthesis methods of graphene, graphene oxide (GO), reduced graphene oxide (rGO) as well as epoxy resin (EP) are summarized in detail. 2D graphene and its derivatives were synthesized and prepared as barrier coating for OLED. Modified Hummer's method was adopted for the synthesis of GO and solution mixing method was selected to prepare GO/EP, rGO/EP nanocomposite during the experiment. The solution is then spin coated on glass and flexible substrates. By adjusting the rotating speed of spin coater, the controlling of film thickness in nanoscale is realized and verified using profiler. All of the prepared films demonstrate high transmittance (>96%) at visible light range. FTIR confirmed the success synthesis of graphene oxide. Compared with graphene oxide, reduced graphene oxide shows higher contact angle even it is difficult to be dispersed. SEM was used to check the surface morphology illustrated that the prepared barrier coatings are flat and without many pin holes. The results indicate that many of graphene's superior properties have

been saved to the GO/EP and rGO/EP nanocomposites film, which make this encapsulation technology attractive and promising.

In the future, the improved preparation method of both GO/EP and rGO/EP nanocomposites for better dispersion can be expected, giving the material better interface compatibility. More material characterization technology should be applied to measure the properties of films in a more comprehensive way. Water Vapour Transmission Rate (WVTR), as the most important parameter to measure the gas barrier performance of the film, should be given priority. GO/EP or rGO/EP nanocomposites with different contents can be prepared to study the effect of GO/rGO content on the properties of the nanocomposites.

6. Potential applications and socio-economic impact

This section is described detailly in the previous chapters and will not be covered too much here. In conclusion, the results indicate that many of graphene's superior properties have been saved to the GO/EP and rGO/EP nanocomposites film, which make this encapsulation technology attractive and promising. After possible improvements technology, the whole production process is easily accessible and has the potential of mass production in industry.

Word Count: *11644* *(The title page, acknowledgements, table of contents, footnotes, figures and tables with their captions, references, appendix, titles and subtitles are not included.)*

References:

1. Marsh, K.; Bugusu, B., Food packaging—roles, materials, and environmental issues. J Food Sci 2007, 72 (3), 2007.
2. Arora, A.; Padua, G., Review: nanocomposites in food packaging. J Food Sci 2010, 75 (1), 2010.
3. Carrera, M. C.; Erdmann, E.; Destéfanis, H. A., Barrier Properties and Structural Study of Nanocomposite of HDPE/Montmorillonite Modified with Polyvinylalcohol. Journal of Chemistry, 1-7, 2013.
4. Jiang, T.; Kuila, T.; Kim, N. H.; Lee, J. H., Effects of surface-modified silica nanoparticles attached graphene oxide using isocyanate-terminated flexible polymer chains on the mechanical properties of epoxy composites. Journal of Materials Chemistry A, 2 (27), 2014.
5. Duncan, T. V., Applications of nanotechnology in food packaging and food safety: barrier materials, antimicrobials and sensors. J Colloid Interface Sci, 363 (1), 1-24, 2011.
6. Huang, H.-D.; Ren, P.-G.; Xu, J.-Z.; Xu, L.; Zhong, G.-J.; Hsiao, B. S.; Li, Z.-M., Improved barrier properties of poly(lactic acid) with randomly dispersed graphene oxide nanosheets. Journal of Membrane Science, 464, 2014.
7. Moller, M. W.; Kunz, D. A.; Lunkenbein, T.; Sommer, S.; Nennemann, A.; Breu, J., UV-cured, flexible, and transparent nanocomposite coating with remarkable oxygen barrier. Advanced Materials, 24 (16), 2012.
8. Choudalakis, G.; Gotsis, A. D., Permeability of polymer/clay nanocomposites: A review. European Polymer Journal, 45 (4), 2009.
9. Chen, B.; Evans, J. R.; Greenwell, H. C.; Boulet, P.; Coveney, P. V.; Bowden, A. A.; Whiting, A., A critical appraisal of polymer–clay nanocomposites. Chem Soc Rev, 37 (3) 568-594, 2008.
10. Sinha Ray, S.; Okamoto, M., Polymer/layered silicate nanocomposites: a review from preparation to processing. Progress in Polymer Science, 28 (11) 1539-1641, 2003.
11. Xiaolin, L.; Xinran, W.; Li, Z.; Sangwon, L.; Hongjie, D. Chemically derived, ultrasmooth graphene nanoribbon semiconductors. Science, 1229–32, 2008.
12. Geim, A. K.; Novoselov, K. S. The rise of graphene. Nat. Mater., 183–191, 2007.
13. Katsnelson, M. I. Graphene: carbon in two dimensions. Mater. Today, 100–127, 2007.
14. Celebrating graphene. Nat. Photonics, (4) 731-731, 2010.
15. Compton, O. C.; Nguyen, S. T. Graphene Oxide, Highly Reduced Graphene Oxide, and Graphene: Versatile Building Blocks for Carbon-Based Materials, 6 (6), 711–723, 2010.
16. Zhao, X.; Zhang, Q. H.; Hao, Y. P.; Li, Y. Z.; Fang, Y.; Chen, D. J. Alternate Multilayer Films of Poly(vinyl alcohol) and Exfoliated Graphene Oxide Fabricated via a Facial Layer-by-Layer Assembly. Macromolecules, 43 (22), 9411–9416, 2010.
17. Gilje, S.; Han, S.; Wang, M.; Wang, K. L.; Kaner, R. B. A chemical route to graphene for device applications. Nano Lett, 7, 3394–3398, 2007.

18. Ye, L.; Ding, P.; Zhang, M.; Qu, B. J. Synergistic effects of exfoliated LDH with some halogen-free flame retardants in LDPE/ EVA/HFMH/LDH nanocomposites. J. Appl. Polym. Sci. 107, 3694–3701, 2008.
19. Marouf, B. T.; Bagheri, R.; Pearson, R. A. Mechanical and thermal properties of montmorillonite-epoxy nanocomposite. Int. J. Mod. Phys. B, 22, 3247–3253, 2008.
20. Rahatekar, S. S.; Zammarano, M.; Matko, S.; Koziol, K. K.; Windle, A. H.; Nyden, M.; Kashiwagi, T.; Gilman, J. W. Effect of carbon nanotubes and montmorillonite on the flammability of epoxy nanocomposites. Polym. Degrad. Stab. 95, 870–879, 2010.
21. Dreyer, D. R.; Park, S.; Bielawski, C. W.; Ruoff, R. S. The chemistry of graphene oxide. Chem. Soc. Rev. 39, 228–240, 2010.
22. Wu, K.; Song, L.; Hu, Y.; Lu, H. D.; Kandola, B. K.; Kandare, E. Synthesis and characterization of a functional polyhedral oligomeric silsesquioxane and its flame retardancy in epoxy resin. Prog. Org. Coat. 65 (4), 490–497, 2009.
23. Kumar, S. A.; Balakrishnan, T.; Alagar, A.; Denchev, Z. Development and characterization of silicone/phosphorus modified epoxy materials and their application as anticorrosion and antifouling coatings. Prog. Org. Coat. 55 (3), 207–217, 2006.
24. Das, G.; Karak, N. Thermostable and flame retardant Mesua ferrea L. seed oil based non-halogenated epoxy resin/clay nanocomposites. Prog. Org. Coat. 69 (4), 495–503, 2010.
25. G. Cheng, K.T. Chan, W.P. To, C.M. Che, Color tunable organic lightemitting devices with external quantum efficiency over 20% based on strongly luminescent gold (III) complexes having long-lived emissive excited states, Adv. Mater. 26 2540–2546, 2014.
26. M. Mazzeo, F. Mariano, A. Genco, et al., High efficiency ITO-free flexible white organic light-emitting diodes based on multi-cavity technology, Org. Electron. 14 (11) 2840–2846, 2013.
27. C.H. Lin, Y.C. Chiu, Y. Chi, Y.T. Tao, L.S. Liao, M.R. Tseng, G.H. Lee, Mechanistic investigation of improved syntheses of iridium (III) - based OLED phosphors, Organometallics. 31 (11) 4349–4355, 2012.
28. Z. T. Zhang, et al, A colour-tunable, weavable fibre-shaped polymer light-emitting electrochemical cell. Nature Photonics. 9, 233–238, 2015.
29. C. W. TANG, Multilayer organic photovoltaic elements. U.S. Patent. 4,164,431[P], 1979.
30. S, Reineke, et al. White organic light-emitting diodes with fluorescent tube efficiency. Nature 459, 234–238, 2009.
31. T. H. Han, et al. Extremely efficient flexible organic light-emitting diodes with modified graphene anode. Nature Photonics 6, 105–110, 2012.
32. H. Aziz, Z. D. Popovic, N. X. Hu, A. M. Hor, G. Xu, Degradation Mechanism of Small Molecule–Based Organic Light-Emitting Devices. Science 283, 1900–1902, 1999.

33. Xu, M. S., Xu, J. B., Chen, H. Z. & Wang, M. Nanoscale investigation of moisture-induced degradation mechanisms of tris (8-hydroxyquinoline) aluminum-based organic light-emitting diodes. Journal Of Physics D-Applied Physics 37, 2618–2622, 2004.
34. Yoo, B. M.; Shin, H. J.; Yoon, H. W.; Park, H. B., Graphene and graphene oxide and their uses in barrier polymers. Journal of Applied Polymer Science, 131 (1), 39628, 2014.
35. WANG, F. K., LU, Y. C., Useful lifetime of white OLED under a constant stress accelerated life testing. Optical & Quantum Electronics, 47(2):323-329, 2015.
36. L.M. Do, M. Oyamada, A. Koike, E.M. Han, N. Yamamoto, M. Fujihira, Morphological change in the degradation of Al electrode surfaces of electroluminescent devices by fluorescence microscopy and AFM, Thin Solid Films 273 209–213, 1996.
37. Moro L. L. M., Rutherford N., Chu X., Visser R. J., Graf G. C., Gross M. E., Bennet W. Barix multilayer barriers: A key enabler for protecting OLED displays and flexible organic devices. Proceedings of International Meeting on Information Display, 616- 619, 2006.
38. M.S. Weaver, L.A. Michalski, K. Rajan, M.A. Rothman, J.A. Silvernail, J.J. Brown, P.E. Burrows, G.L. Graff, M.E. Gross, M. Zumhoff, Organic light-emitting devices with extended operating lifetimes on plastic substrates, Appl. Phys. Lett. 81 2929–2931, 2002.
39. Z. Cheng, H. R. Wang, X. Wang, P. Chen, Y. F. Liu, H. Y. Zhao, Y. Zhao, Y. Duan. Low-temperature remote plasma enhanced atomic layer deposition of ZrO2/zircone nanolaminate film for efficient encapsulation of flexible organic light-emitting diodes. Nature, Scientific Reports, 7:40061, 2017.
40. YU D., YANG Y. Q., CHEN Z., et al. Recent progress on thin-film encapsulation technologies for organic electronic devices. Opt Commun 362: 43-49, 2016.
41. RIEDEL D., DLUGOSCH J., WEHLUS T., et al. Extracting and shaping the light of OLED devices [C]. Organic Light Emitting Materials and Devices XIX. International Society for Optics and Photonics:1364, 2015.
42. SU S. H., HOU C. C., SHIEH R. S., et al. Enhancing Efficiency of Organic Light-Emitting Diodes Using Lithium-Doped Electron Transport Layer. Japanese Journal of Applied Physics, 47(4):3193-3195, 2008.
43. F.L. Wong, M.K. Fung, S.L. Tao, S.L. Lai, W.M. Tsang, K.H. Kong, W.M. Choy, C.S. Lee, S.T. Lee, Long-lifetime thin-film encapsulated organic light-emitting diodes, J. Appl. Phys. 104 014509, 2008.
44. J. Granstrom, J.S. Swensen, J.S. Moon, G. Rowell, J. Yuen, A.J. Heeger, Encapsulation of organic light-emitting devices using a perfluorinated polymer, Appl. Phys. Lett. 93 193304, 2008.
45. KALYANI N T., DHOBLE S. J., Novel materials for fabrication and encapsulation of OLEDs. Renewable & Sustainable Energy Reviews, 44:319-347, 2015.
46. MORO L., BOESCH D., ZENG X., OLED Encapsulation [M]. OLED Fundamentals, 2015.

47. ZHANG J., ZHANG F. H., ZHANG L., et al. Effect of Cover Glass on OLED Encapsulation Performance. Chinese Journal of Liquid Crystals & Displays, 27(5):628-632, 2012.
48. SANGEE Ko Park, JIYOUNG Oh, HWANG Chiun, et al. Ultra-thin film encapsulation of OLED on plastic substrate. ETRI Journal 27 5(2005-10-14), 27(5): 545-550, 2005.
49. Y. B. Cui, S. I. Kundalwal, S. Kumar. Gas Barrier Performance of Graphene/Polymer Nanocomposites, Masdar Institute of Science and Technology, P.O. Box 54224, Abu Dhabi, U.A.E.
50. KALAITZIDOU K, FUKUSHIMA H, DRZAL L T.Multifunctional polypropylene composites produced by incorporation of exfoliated graphite nanoplatelets. Carbon, 45 (7): 1446-1452,2007.
51. PARK E. K., KIM S., HEO J., et al. Electrical evaluation of crack generation in SiNx, and SiOxNy, thin-film encapsulation layers for OLED displays. Applied Surface Science, 370:126-130, 2016.
52. YAMASHITA K., MORI T., MIZUTANI T. Encapsulation of organic light-emitting diode using thermal chemicalvapour-deposition polymer film. Journal of physics D: Applied physics, 34(5): 740, 2001.
53. Chwang, A. B. et al. Thin film encapsulated flexible organic electroluminescent displays. Applied Physics Letters 83, 413–415, 2003.
54. Ghosh, A. P., Gerenser, L. J., Jarman, C. M. & Fornalik, J. E. Thin-film encapsulation of organic light-emitting devices. Applied Physics Letters 86, 1–3, 2005.
55. Kim, L. H. et al. Al2O3/TiO2 nanolaminate thin film encapsulation for organic thin film transistors via plasma-enhanced atomic layer deposition. ACS Appl Mater Interfaces 6, 6731–6738, 2014.
56. Li, M. et al. Facilitation of transparent gas barrier using SiNx/a-IZO lamination for organic light emitting diodes. Organic Electronics 24, 57–64, 2015.
57. Drahushuk, L. W.; Strano, M. S. Langmuir 28, 16671, 2012.
58. Novoselov K S, Geim A K, Morozov S V, Jiang D, Zhang Y, Dubonos S V, Grigorieva IV and Firsov A A. Electric Field Effect in Atomically Thin Carbon Films. Science,306: 666-669, 2004.
59. Nilsson, L.; Andersen, M.; Balog, R.; Lægsgaard, E.; Hofmann, P.; Besenbacher, F.; Hammer, B.; Stensgaard, I.; Hornekaer, L. Am. Chem. Soc. Nano 6, 10258, 2012.
60. Bunch, J. S.; Verbridge, S. S.; Alden, J. S.; Van Der Zande, A. M.; Parpia, J. M.; Craighead, H. G.; McEuen, P. L. Nano Lett. 8, 2458, 2008.
61. O. Sneh, R.B.C. lark-Phelps, A.R. Londergan, J. Winkler, T.E. Seidel, Thin film atomic layer deposition equipment for semiconductor processing, Thin Solid Films 402, 248–261, 2002.
62. PENG Rong. Research on packaging methods based on OLED devices. Electronics & Packaging, 20(5): 050101, 2020.
63. J. Meyer, P. Goerrn, F. Bertram, S. Hamwi, T. Winkler, H.H. Johannes, T. Weimann, P. Hinze, T. Riedl, W. Kowalsky, Al2O3/ ZrO2Nanolaminates as ultrahigh gas-diffusion barriers – a strategy for reliable encapsulation of organic electronics, Adv. Mater. 21, 1845–1849, 2009.
64. M. Putkonen, J. Harjuoja, T. Sajavaara, L. Niinistö, Atomic layer deposition of WO3 thin films using W(CO)6 and O3 precursors, J. Mater. Chem. 129 (664), 2007.

65. Y. Duan, F.B. Sun, Y.Q. Yang, P. Chen, D. Yang, Y.H. Duan, X. W., Thinfilm barrier performance of zirconium oxide using the lowtemperature atomic layer deposition method, ACS Appl. Mater. Interfaces 6 3799–3804, 2010.
66. M. Putkonen, J. Harjuoja, T. Sajavaara, L. Niinistö, Atomic layer deposition of WO3 thin films using W(CO)6 and O3 precursors, J. Mater. Chem. 129 664, 2007.
67. K.B. Klepper, O. Nilsen, H. Fjellvåg, Deposition of thin films of organic–inorganic hybrid materials based on aromatic carboxylic acids by atomic layer deposition, Dalton Trans. 39 11628, 2010.
68. K. Neyts, Simulation of light emission from thin-film microcavities, J. Opt. Soc. Am. A: 15 962–971, 1998.
69. HILTNER A, LIU R Y F, HU Y S, BAER E.Oxygen transport as a solid-state structure probe for polymeric materials: A review. Journal of Polymer Science Part B: Polymer Physics, 43 (9): 1047-1063 ,2005.
70. Nielsen, L. E. J. Macromol. Sci. Chem. 1, 929, 1967.
71. LEE C, WEI X, KYSAR J W, HONE J. Measurement of the Elastic Properties and Intrinsic Strength of Monolayer Graphene. Science, 321 (5887): 385-388, 2008.
72. TAN B, THOMAS N L. A review of the water barrier properties of polymer/clay and polymerigraphene nanocomposites. Journal of Membrane Science, 514: 595-612, 2016.
73. BALANDIN A A, GHOSH S, BAO W, CALIZO I, TEWELDEBRHAN D, MIAO F, LAU C N. Superior thermal conductivity of single-Layer graphene. Nano Letters, 8 (3): 902-907, 2008.
74. A.A. Dameron, D. Seghete, B.B. Burton, S.D. Davidson, A.S. Cavanagh, J.A. Bertrand, S.M. George, Molecular layer deposition of alucone polymer films using trimethylaluminum and ethylene glycol, Chem. Mater. 20 3315, 2008.
75. A. Sood, P. Sundberg, J. Malm, M. Karppinen, Layer-by-layer deposition of Ti–4,40 -oxydianiline hybrid thin films, Appl. Surf. Sci. 257 6435, 2011.
76. Lerf A, He H, Forster M, et al. Structure of graphite oxide revisted. J Phys Chem B, 102: 4477-4482,1998.
77. Morimune, S.; Nishino, T.; Goto, T., Ecological Approach to Graphene Oxide Reinforced Poly (methyl methacrylate) Nanocomposites. ACS Applied Materials & Interfaces 4 (7), 3596-3601, 2012.
78. Brodie B C. On the Atomic Weight of GraphiteJ]. Philos. Trans. R. Soc. London,149: 249-259, 1859.
79. Staudenmaier L. Verfahren zur Darstellung der GraphitsäurejJ]. Ber. Dtsch. C'hem. Ges., 31: 1481-1487,1898.
80. Hummers W S and Offeman R E. Preparation of Graphitic Oxide. J. Am. Chem. Soc., 80: 1339,1958.
81. Lakshminarayanan P V, Toghiani H and Jr C U P. Nitric acid oxidation of vapor grown carbon nanofibers. Carbon,42: 2433-2442, 2004.
82. Koch K R and Krause P F. Oxidation by Mn207: An impressive demonstration of the powerful oxidizing property of dimanganeseheptoxide. J. Chem. Ed., 59, 973-974, 1982.

83. Tromel M and Russ M. Dimanganheptoxid zur selektiven Oxidation organischerSubstrate. Angew. Chem., 99: 1037-1038, 1987.
84. Terrones, M.; Martin, O.; Gonzalez, M.; Pozuelo, J.; Serrano, B.; Cabanelas, J. C.; Vega-Diaz, S. M.; Baselga, J. Adv. Mater. 23, 5302, 2011.
85. Kovtyukhova, N. I.; Ollivier, P. J.; Martin, B. R.; Mallouk, T. E.; Chizhik, S. A.; Buzaneva, E. V.; Gorchinskiy, A. D. Chem. Mater. 11, 771, 1999.
86. Marcano, D. C.; Kosynkin, D. V.; Berlin, J. M.; Sinitskii, A.; Sun, Z.; Slesarev, A.; Alemany, L. B.; Lu, W.; Tour, J. M. Am. Chem. Soc. Nano 4, 4806, 2010.
87. Becerril, H. A.; Mao, J.; Liu, Z.; Stoltenberg, R. M.; Bao, Z.; Chen, Y. Evaluation of solution-processed reduced graphene oxide films as transparent conductors. ACS Nano 2, 463–470, 2008.
88. Tung, V. C.; Allen, M. J.; Yang, Y.; Kaner, R. B. High throughput solution processing of large-scale graphene. Nat. Nanotechnol., 4, 25–29, 2009.
89. Wang, G. A.; Cheng, W. M.; Tu, Y. L.; Wang, C. C.; Chen, C. Y. Characterizations of a new flame-retardant polymer. Polym. Degrad. Stab. 91, 3344–3353, 2006.
90. Wu, K.; Song, L.; Hu, Y.; Lu, H. D.; Kandola, B. K.; Kandare, E. Synthesis and characterization of a functional polyhedral oligomeric silsesquioxane and its flame retardancy in epoxy resin. Prog. Org. Coat. 65, 490–497, 2009.
91. Stankovich, S.; Piner, R. D.; Chen, X.; Wu, N.; Nguyen, S. B. T.; Ruoff, R. S. J. Mater. Chem. 16, 155, 2006.
92. Gorrasi, G.; Tortora, M.; Vittoria, V.; Pollet, E.; Lepoittevin, B.; Alexandre, M.; Dubois, P. Polymer 44, 2271, 2003.
93. Zhang R, Hu Y. Preparation and Combustion Properties of Flame Retardant Styrene-Butyl Acrylate Copolymer/Graphite Oxide Nanocomposites. Macromol. Mater. Eng.,289: 355-359, 2004.
94. Dasari A, Yu ZZ, Mai Y W, Cai G P and Song H H. Roles of graphite oxide, clay and POSS during the combustion of polyamide 6. Polymer, 50: 1577-1587, 2009.
95. Han Z D, Wang J Q. The combustion behavior of polyacrylate ester/graphite oxidecomposites. Polym. Adv. Techol, 17: 335-340., 2006.
96. Shi L, Li Z M, Xie B H, Hua J, Tian C R, Yang M B. Flame retardancy of different-sized expandable graphite particles for high-density rigid polyurethane foams. Polym. Int., 55: 862-871,2006.
97. Chae H K, Siberio-Perez D Y, Kim J, Go Y, Eddaoudi M, Matzger A J, Keeffe M Oand Yaghi O Y. A route to high surface area, porosity and inclusion of large molecules in crystals. Nature, 427: 523-527, 2004.
98. Wang G Yang Y, Park J, Gou B, Wang B, Liu H and Yao J. J Facile Synthesis and Characterization of Graphene Nanosheets. J. Phys. Chem. C, 112: 8192-8195, 2008.
99. Wu Z S, Ren W, Gao L, Liu B, Jiang C and Cheng H M. Synthesis of high-quality graphene with a pre-determined number of layers. Carbon, 47: 493-499, 2009.

100. Guo Y Q, Bao C L, Song L, Yuan B H, Hu Y. In Situ Polymerization of Graphene, Graphite Oxide, and Functionalized Graphite Oxide into Epoxy Resin and Comparison Study of On-the-Flame Behaviour. Ind. Eng. Chem. Res. 50, 7772, 2011.

101. Mesfin, H. M.; Baudouin, A. C.; Hermans, S.; Delcorte, A.; Huynen, I.; Bailly, C., Frequency selective microwave absorption induced by controlled orientation of graphene-like nanoplatelets in thin polymer films. Applied Physics Letters, 105 (10), 2014.

102. Saravanan, N.; Rajasekar, R.; Mahalakshmi, S.; Sathishkumar, T. P.; Sasikumar, K. S. K.; Sahoo, S., Graphene and modified graphene-based polymer nanocomposites - A review. Journal of Reinforced Plastics and Composites, 33 (12), 1158-1180, 2014.

103. Liu, W.; Zhou, R.; Zhou, D.; Ding, G.; Soah, J. M.; Yue, C. Y.; Lu, X., Lignin-assisted direct exfoliation of graphite to graphene in aqueous media and its application in polymer composites. Carbon, 83, 188-197, 2015.

104. Zaman, I.; Kuan, H.-C.; Dai, J.; Kawashima, N.; Michelmore, A.; Sovi, A.; Dong, S.; Luong, L.; Ma, J., From carbon nanotubes and silicate layers to graphene platelets for polymer nanocomposites. Nanoscale, 4 (15), 4578-4586, 2012.

105. Yeh, J. M.; Huang, H. Y.; Chen, C. L.; Su, W. F.; Yu, Y. H., Siloxane-modified epoxy resin–clay nanocomposite coatings with advanced anticorrosive properties prepared by a solution dispersion approach. Surface and Coatings Technology, 200 (8), 2753-2763, 2006.

106. Li, D.; Muller, M. B.; Gilje, S.; Kaner, R. B.; Wallace, G. G. € Nat. Nanotechnol, 3, 101, 2008.

107. Fang, M.; Wang, K. G.; Lu, H. B.; Yang, Y. L.; Nutt, S. Covalent polymer functionalization of graphene nanosheets and mechanical properties of composites. J. Mater. Chem. 19, 7098–7105, 2009.

108. Li, D.; Muller, M. B.; Gilje, S.; Kaner, R. B.; Wallace, G. G. Processable aqueous dispersions of graphene nanosheets. Nat. Nanotechnol. 3 (2), 101–105, 2008.

Appendix 1: Epoxy Resin Specification

TECHNICAL DATASHEET

DELO

DELO® KATIOBOND® LP655

modified epoxy resin | 1C | UV- / VIS-curing

free of solvents | thixotropic | high water vapor barrier

Special features of product
- compliant with RoHS Directive 2015/863/EU

Typical area of use
- -40 - 120 °C

Curing

Suitable lamp types	LED 365 nm, LED 400 nm, UVA	
Typical irradiation time		
intensity 200 mW/cm² LED 400 nm	20	s

Processing

Typical adhesive application	needle dispensing	
Conditioning time (typical)		
when stored in cold conditions in containers up to 1,000 ml	6	h
when stored in cold conditions in containers up to 10 l	12	h
Processing time		
at rt approx. +23 °C	28	d
Storage life in unopened original container		
at 0 °C to +10 °C	6	month(s)

Technical properties

Transparency	translucent
Color in cured condition in 0.1 mm layer thickness	colorless
Transparency in cured condition in 0.1 mm layer thickness	transparent

Color in cured condition in 1 mm layer thickness	yellowish	

Parameters

Density *DELO Standard 13 / liquid*	1.38	g/cm³
Viscosity *liquid / Rheometer / Shear rate: 10 1/s*	12000	mPa·s
Thixotropy index *liquid / Rheometer*	1.3	
Minimum irradiation time *DELO Standard 37 / DSC / 400 nm / 200 mW/cm² / Measuring temperature: 30 °C*	10	s
Maximum curable layer thickness *DELO Standard 20 / **White substrate** / 400 nm / 200 mW/cm² / 20 s / Plus / at approx. +23 °C / 24 h*	0.4	mm
Maximum curable layer thickness *DELO Standard 20 / **White substrate** / 400 nm / 200 mW/cm² / 60 s / Plus / at approx. +23 °C / 24 h*	0.7	mm
Compression shear strength *DELO Standard 5 / **Glass** / **Al** / 400 nm / 200 mW/cm² / 20 s / Plus / at approx. +23 °C / 24 h*	12	MPa
Compression shear strength *DELO Standard 5 / **Glass** / **Glass** / 400 nm / 200 mW/cm² / 20 s / Plus / at approx. +23 °C / 24 h*	9	MPa
Compression shear strength *DELO Standard 5 / **Glass** / **PC** / 400 nm / 200 mW/cm² / 20 s / Plus / at approx. +23 °C / 24 h*	3	MPa
Tensile strength *Based on DIN EN ISO 527 / 400 nm / 200 mW/cm² / 60 s / Plus / at approx. +23 °C / 24 h*	22	MPa
Elongation at tear *Based on DIN EN ISO 527 / 400 nm / 200 mW/cm² / 60 s / Plus / at approx. +23 °C / 24 h*	1	%
Young's modulus *DMTA / 400 nm / 200 mW/cm² / 60 s / Plus / at approx. +23 °C / 24 h / Type of storage: Temp. / Storage temperature: 205 °C / Duration: 30 min*	5300	MPa
Shore hardness D *Based on DIN EN ISO 868 / 400 nm / 200 mW/cm² / 60 s / Plus / at approx. +23 °C / 24 h*	84	
Glass transition temperature *DMTA / 400 nm / 200 mW/cm² / 60 s / Plus / at approx. +23 °C / 24 h / Type of storage: Temp. / Storage temperature: 205 °C / Duration: 30 min*	183	°C

Coefficient of linear expansion *DELO Standard 26 / TMA / Evaluation T: 30 °C - 40 °C / 400 nm / 200 mW/cm² / 60 s / Plus / at approx. +23 °C / 24 h*	45	ppm/K
Coefficient of linear expansion *DELO Standard 26 / TMA / Evaluation T: 140 °C - 150 °C / 400 nm / 200 mW/cm² / 60 s / Plus / at approx. +23 °C / 24 h*	132	ppm/K
Shrinkage *DELO Standard 13 / 400 nm / 200 mW/cm² / 60 s / Plus / at approx. +23 °C / 24 h*	2.4	vol. %
Permeation *Layer thickness: 500 µm / 400 nm / 200 mW/cm² / 20 s / Plus / at approx. +23 °C / 24 h / Type of storage: Constant climate / Storage temperature: 60 °C / Humidity: 90 % / Duration: 24 h*	6	g/(m²·24h)
Relative permittivity *1 MHz*	3.1	
Relative permittivity *10 MHz*	3.2	
Relative permittivity *100 MHz*	3.1	
Relative permittivity *1000 MHz*	3	

Converting table

°F	= (°C x 1.8) + 32	1 MPa	= 145.04 psi
1 inch	= 25.4 mm	1 GPa	= 145.04 ksi
1 mil	= 25.4 µm	1 cP	= 1 mPa·s
1 oz	= 28.3495 g	1 N	= 0.225 lb

General curing and processing information

The curing time stated in the technical data was determined in the laboratory. It can vary depending on the adhesive quantity and component geometry and is therefore a reference value.Increasing or decreasing the curing temperature and / or irradiation intensity and / or irradiation time shortens or prolongs the curing time and can lead to changed physical properties.All curing or light fixation parameters depend on material thickness and absorption, adhesive layer thickness, lamp type and distance between lamp and adhesive layer.Curing until final strength proceeds within 24 hours at room temperature.High temperatures during or after curing can lead to post-crosslinking of the adhesive which influences the physical properties of the bond.Values measured after 24 h at approx. 23 °C / 50 % r.h., unless otherwise specified.

General

The data and information provided are based on tests performed under laboratory conditions. Reliable information about the behavior of the product under practical conditions and its suitability for a specific

purpose cannot be concluded from this. It is the customer's responsibility to test the suitability of a product for the intended purpose by considering all specific requirements and by applying standards the customer deems suitable (e. g. DIN 2304-1). Type, physical and chemical properties of the materials to be processed with the product, as well as all actual influences occurring during transport, storage, processing and use, may cause deviations in the behavior of the product compared to its behavior under laboratory conditions. All data provided are typical average values or uniquely determined parameters measured under laboratory conditions. The data and information provided are therefore no guarantee for specific product properties or the suitability of the product for a specific purpose.
Nothing contained herein shall be construed to indicate the non-existence of any relevant patents or to constitute a permission, encouragement or recommendation to practice any development covered by any patents, without permission of the owner of this patent.
All products provided by DELO are subject to DELO's General Terms of Business. Verbal ancillary agreements are deemed not to exist.

Instructions for use

You can find further details in the instructions for use.

The instructions for use are available on www.DELO-adhesives.com.

We will be pleased to send them to you on demand.

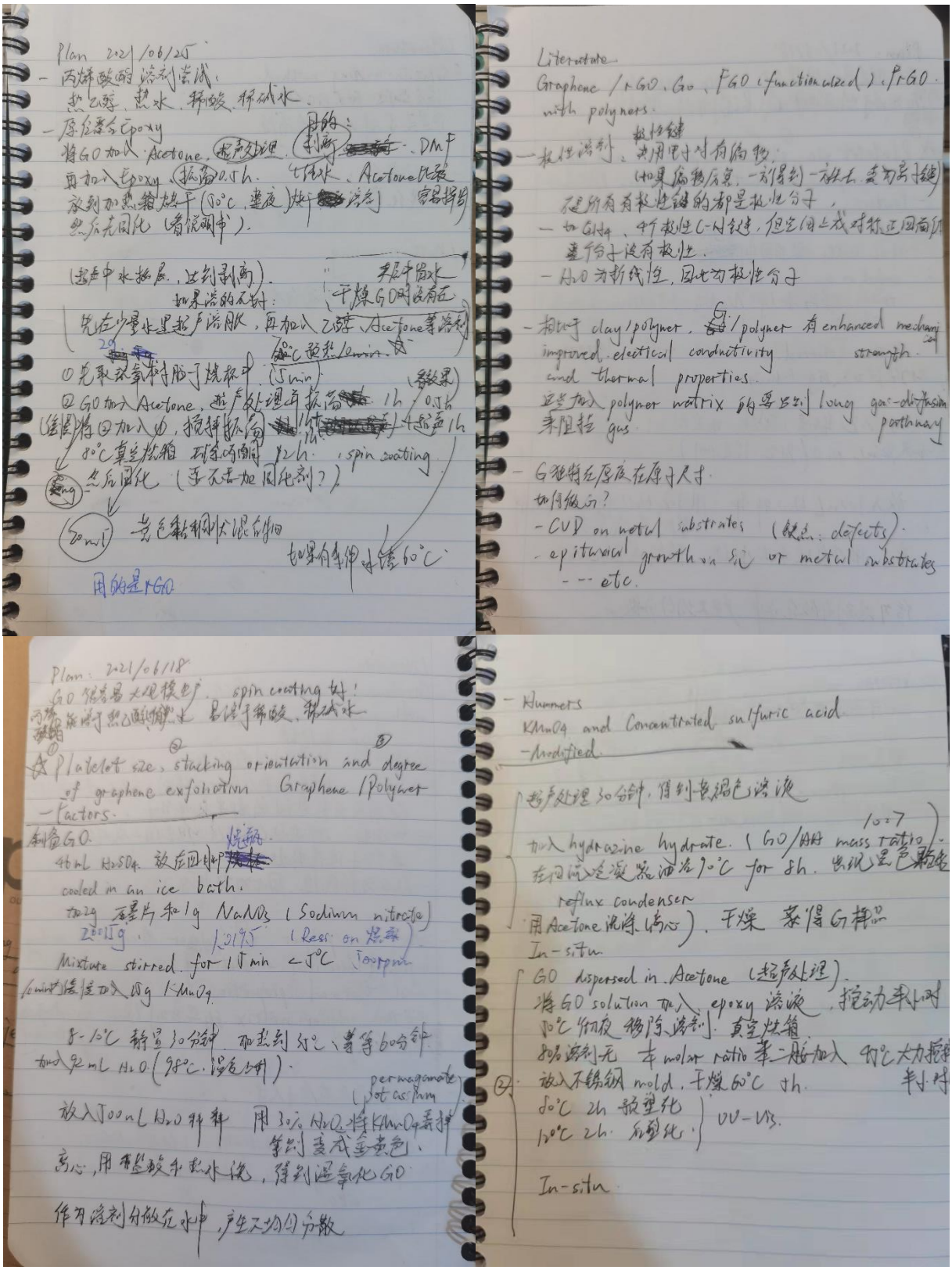
Occupational health and safety

See material safety data sheet.

Specification

Nothing contained in this Technical Datasheet shall be interpreted as any express warranty or guarantee. This Technical Datasheet is for reference only and does not constitute a product specification. Please ask our responsible Sales Engineer for the applicable product specification which includes defined ranges. DELO is neither liable for any values and content of this Technical Datasheet nor for oral or written recommendations regarding the use, unless otherwise agreed in writing. This limitation of liability is not applicable for damages resulting from intent, gross negligence or culpable breach of cardinal obligations, nor shall it apply in case of death or personal injury or in case of liability under any applicable compulsory law.

Appendix 2: Screenshots of 5 full pages



Plan 2021/06/25
- 丙烯酸酯溶剂法：
热乙醇、热水、稀硫酸、移液水。
- 原位聚合 Epoxy
将GO加入 Acetone，超声处理（目的：剥离）~~DMF~~
再加入 Epoxy，搅拌0.5h。七水、Acetone比较容易挥发
放到加热箱烘干（80°C，速度）~~烘~~
然后光固化（看说明书）。

（超声中水振荡，出到剥离）。
如果溶的不好：
先在少量水里超声溶胀，再加入乙醇、Acetone等溶剂
① 先取浓氧化石墨烯于烧杯中（5min）
② GO加入 Acetone，超声处理 1h，搅拌振荡 1h，超声 1h
80°C真空烘箱 时间 12h，spin coating
然后固化（要不要加固化剂？）
50ml 一点色黏稠状混合物
用的是rGO

Literature
Graphene / rGO、Go、FGO（functionalized）、PrGO
with polymers.
- 极性溶剂，适用把对有偶极（极性键）
（如果偶极后来，一对得到一对共用电子对）
不是所有有极性键的都是极性分子，
- 如 CH_4，4个极性C-H键，但空间上成对称正四面体
整个分子没有极性。
- H_2O 为折线性，因此为极性分子

- 相对于 clay/polymer，G/polymer 有 enhanced mechanical strength，improved electrical conductivity and thermal properties.
当加入 polymer matrix 的要达到 long gas-diffusion pathway 来阻挡 gas
- G独特在原位在原子尺寸
如何做？
- CVD on metal substrates（缺点：defects）
- epitaxial growth on Si or metal substrates
--- etc.

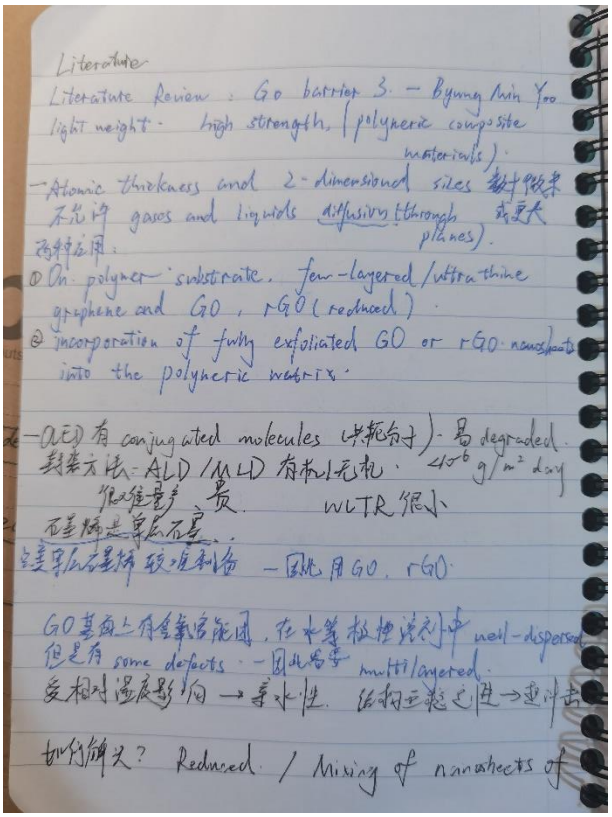
Plan: 2021/06/18
GO 能容易大规模生产，spin coating 好！
Platelet size, stacking orientation and degree of graphene exfoliation Graphene/Polymer factors.

制备GO
46mL H_2SO_4 放在四口烧瓶 cooled in an ice bath.
加2g 石墨片和1g $NaNO_3$（Sodium nitrate）
Mixture stirred for 15min <3°C
缓慢加入3g $KMnO_4$
8-10°C 静置30分钟，加热到35°C，静置60分钟
加入5mL H_2O（98°C，慢慢加）。
放入100mL H_2O 稀释 用30% H_2O_2 将 $KMnO_4$ 去掉（permagamate 或 MnO_2）
到变成金黄色。
离心，用稀盐酸和热水洗，得到还原化GO
作为溶剂分散在水中，产生之为均分散

- Hummers
$KMnO_4$ and Concentrated sulfuric acid
-Modified

超声处理30分钟，得到黄褐色溶液
加入 hydrazine hydrate（GO/肼 mass ratio 1:7）
在回流冷凝管油浴 95°C for 5h，出现黑色絮状
reflux condenser
用 Acetone 洗涤（离心），干燥 获得GO样品
In-situ
GO dispersed in Acetone（超声处理）
将GO solution 加入 epoxy 溶液，搅动半小时
80°C 抽取 溶剂，真空烘箱
80°C 除溶剂无 本 molar ratio 苯二胺加入 90°C 大力搅拌半小时
② 放入不锈钢 mold，干燥 60°C 5h
80°C 2h 预固化
120°C 2h 后固化
UV-Vis.

In-situ



Appendix 3: Supervision Log

Student Name: Ziyan WU

Date of Meeting: Monday, 24 May 2021

Section to be completed by the student

Summary of progress made:

Discuss for the choice of material.

Section to be completed by the supervisor

Feedback from the supervisor:

Read more recommended literature. Try to do some scientific comparison.

Suggestion for next steps:

Please follow as what we have discussed.

Student signature: Ziyan WU

Supervisors Name: Mingqing, WANG Mingqing Wang

Student Name: Ziyan WU

Date of Meeting: Friday, 4 June 2021

Section to be completed by the student

Summary of progress made:

Making the slides for interim presentation

Highlight any issues/problems encountered that need help:

Advice for interim presentation

Section to be completed by the supervisor

Feedback from the supervisor:

Too many words on it, try to put some diagrams for illustration

Suggestion for next steps:

Make sure you presented the key information within 5min

Student signature: Ziyan WU

Supervisors Signature:

Supervisors Name: Mingqing, WANG Mingqing Wang

Student Name: Ziyan WU

Date of Meeting: Friday, 18 June 2021

Section to be completed by the student

Summary of progress made:

Read many literatures related to organic/inorganic multilayer film

Highlight any issues/problems encountered that need help:

Do not know the feasibility of the plan

Section to be completed by the supervisor

Feedback from the supervisor:

Good effort, ALD and MLD is not available and difficult to operate

Suggestion for next steps:

Try to find graphene/polymer nanocomposites related literature and read

Student signature: Ziyan WU

Supervisors Signature:

Supervisors Name: Mingqing, WANG Mingqing Wang

Student Name: Ziyan WU

Date of Meeting: Friday, 2 July 2021

Section to be completed by the student

Summary of progress made:

Start to work with synthesis of graphene oxide

Highlight any issues/problems encountered that need help:

Advice for the methodology of GO synthesis

Section to be completed by the supervisor

Feedback from the supervisor:

The student has read a lot of references, a specific experimental plan with procedures is needed

Suggestion for next steps:

Finish the COSHH and safety form since the experiment is risky

Student signature: Ziyan WU

Supervisors Signature:

Supervisors Name: Mingqing, WANG Mingqing Wang

Student Name: Ziyan WU

Date of Meeting: Friday, 16 July 2021

Section to be completed by the student

Summary of progress made:

Tried the synthesis of GO

Highlight any issues/problems encountered that need help:

Advices for choice of polymer matrix

Section to be completed by the supervisor

Feedback from the supervisor:

Need to read more literatures related to polymer based-nanocomposite and then make a plan on preparation of polymer/GO composite.

Suggestion for next steps:

There are two types of polymers available (acrylic ester and epoxy resin) in the lab, read more about these.

Student signature: Ziyan WU

Supervisors Signature:

Supervisors Name: Mingqing, WANG

Mingqing Wang

Student Name: Ziyan WU

Date of Meeting: Friday, 30 July 2021

Section to be completed by the student

Summary of progress made:

Have tried to prepare of polyacrylic ester / Graphene mixture, mixed solution is obtained.

Highlight any issues/problems encountered that need help:

Do not know which preparation method of nanocomposite is suitable

Section to be completed by the supervisor

Feedback from the supervisor:

Good progress. Melting process is not suitable since the film should be prepared on flexible substrates and the temperature is too high

Suggestion for next steps:

Try solution mixing method. It is easy to operate and can achieve well dispersed solution.

Student signature: Ziyan WU

Supervisors Signature:

Supervisors Name: Mingqing, WANG Mingqing Wang

Student Name: Ziyan WU

Date of Meeting: Friday, 13 August 2021

Section to be completed by the student

Summary of progress made:

Use Acetone as the solvent and have prepared for coating film

Highlight any issues/problems encountered that need help:

Advice for the other choice of solvent for better dispersion

Section to be completed by the supervisor

Feedback from the supervisor:

Try isopropanol.

Suggestion for next steps:

Graphene oxide can be easily dispersed in polar solvents. More attempts are needed for different solvent.

Student signature: Ziyan WU

Supervisors Signature:

Supervisors Name: Mingqing, WANG Mingqing Wang

Student Name: Ziyan WU

Date of Meeting: Friday, 27 August 2021

Section to be completed by the student

Summary of progress made:

Have made some samples of GO/EP films on glass substrates

Highlight any issues/problems encountered that need help:

Advices for the further step and objective of experiment

Section to be completed by the supervisor

Feedback from the supervisor:

Try reduce Graphene Oxide and set control groups.

Suggestion for next steps:

Read more literature and figure out what data is needed.

Student signature: Ziyan WU

Supervisors Signature:

Supervisors Name: Mingqing, WANG Mingqing Wang

Student Name: Ziyan WU

Date of Meeting: Tuesday, 31 August 2021

Section to be completed by the student

Summary of progress made:

Finished the preparation and have finished the characterization.

Highlight any issues/problems encountered that need help:

Advices for the results part of the dissertation.

Section to be completed by the supervisor

Feedback from the supervisor:

Good Progress

Suggestion for next steps:

Explore more on the difference in microstructure and properties between GO and rGO nanocomposites.

Student signature: Ziyan WU

Supervisors Signature:

Supervisors Name: Mingqing, WANG Mingqing Wang

Student Name: Ziyan WU

Date of Meeting: Monday, 6 September 2021

Section to be completed by the student

Summary of progress made:

Revised and checked the whole dissertation

Highlight any issues/problems encountered that need help:

Confirm the final version of the dissertation

Section to be completed by the supervisor

Feedback from the supervisor:

Well done.Format the figures and remove some photos for general equipment such as hotplate and spin coating…

Suggestion for next steps:

Proof-read the draft for minor grammar and spelling mistake. Make sure you submit all of the required documents in one pdf file.

Student signature: Ziyan WU

Supervisors Signature:

Supervisors Name: Mingqing, WANG Mingqing Wang